The Hox Gene, *abdominal A* controls timely mitotic entry of neural stem cell and their growth during CNS development in *Drosophila*

Papri Das[a], Smrithi Murthy[b], Eshan Abbas[c], Kristin White[d], Richa Arya[a*]

[a]Cytogenetics Laboratory, Department of Zoology, Institute of Science, Banaras Hindu University, Varanasi-221005
[b]Ashanagar Phase 2, Mulund (West), Mumbai 400080,
[c]ADP Road, Christianpatty, Nagaon, Assam- 782003, India
[d] MGH/Harvard Medical School,CBRC, Bldg 149, 13th St, Charlestown, MA 02129

*Corresponding author: aryaricha@bhu.ac.in

Running title: *abdA* regulates NSC growth & neurogenesis

Abstract

The size of a cell is important for its function and physiology. Interestingly, size variation can be easily observed in clonally derived embryonic and hematopoietic stem cells. Here, we investigated the regulation of stem cell growth and its association with cell fate. We observed heterogeneous sizes of neuroblasts or neural stem cells (NSCs) in the *Drosophila* ventral nerve cord (VNC). Specifically, thoracic NSCs were larger than those in the abdominal region of the VNC. Our research uncovered a significant role of the Hox gene *abdominal A* (*abdA*) in the regulation of abdominal NSC growth. Developmental expression of AbdA retards their growth and delays mitotic entry compared to thoracic NSCs. The targeted loss of *abdA* enhanced their growth and caused an earlier entry into mitosis with a faster cycling rate. Furthermore, ectopic expression of *abdA* reduced the size of thoracic NSCs and delayed their entry into mitosis. We suggest that *abdA* plays an instructive role in regulating NSC size and exit from quiescence. This study demonstrates for the first time the involvement of *abdA* in NSC fate determination by regulating their growth, entry into mitosis and proliferation rate, and thus their potential to make appropriate number of progeny for CNS patterning.

Key words: *Drosophila*, CNS, Neural stem cells (NSCs), Neuroblasts (NBs), Growth, Mitosis, Proliferation, Hox gene, *abdA*.

Significance statement:

- Understanding the upstream regulation of various aspects of the cell cycle is very important, how cell growth influences the process is largely unknown.
- We found an instructive role of the Hox gene *abdominal A* in maintaining the small size of neural stem cells (NSCs) and limiting their ability to undergo mitosis.
- This mechanism is crucial, as it helps NSCs generate the necessary number of neurons at the appropriate developmental stage, thereby contributing to proper central nervous system patterning.

Introduction

Cell growth is an important parameter that regulates several aspects of its function and fate. The metabolic status, specialized secretion, transport, proliferation, and many other cellular activities depend on cell size **(Cadart et al., 2018; Ginzberg et al., 2018; Kafri et al., 2013; Miettinen & Björklund, 2016).** Although the mechanism of action of crucial cell growth regulating pathways, such as Hippo, Insulin signaling, and PI3K, is known, little is known about the systemic and local cues that determine the growth. Exploring how cell growth and size is regulated in time and space and its linkage with cell fate and function is an exciting area of research from the perspective of development and disease point of view.

Similar to other cells, stem cell populations are heterogeneous in size. Mammalian hematopoietic stem cells (HSCs), which generate diverse types of blood cells, exhibit a large diversity in their size (Lengefeld et al., 2021). An increase in the size of HSCs reduces their stemness and vice versa (Lengefeld et al., 2021). In the *Drosophila* midgut, stem cells differ in shape and size, and produce different progeny in a region-specific manner (Marianes & Spradling, 2013). Gut stem cells produce enterocytes and enteroendocrine cells that are required to produce digestive enzymes and neuropeptides, respectively (Micchelli & Perrimon, 2006; Ohlstein & Spradling, 2007Click or tap here to enter text.). The number of enterocytes and enteroendocrine cells differs among different gut regions (Marianes & Spradling, 2013). Interestingly, the proliferative ability of gut stem cells also differs in a region-specific manner. Stem cells in the posterior part of the gut divide faster than those in the anterior and middle midgut regions (Marianes & Spradling, 2013; Matthews et al., 2009). Furthermore, the synthesis and presence of lipid droplets in posterior midgut stem cells reflect the functional diversity of gut stem cells (Matthews et al., 2009).

Homeotic (Hox) genes are crucial for tissue patterning and in establishing cell segment-specific identity and function (Lewis, 1978; Mann & Morata, 2000). Mutations in Hox genes can transform the identity of one tissue into another (Lewis, 1978). For example, mutations in *Drosophila* Hox genes, *ultrabithorax*, *antennapedia*, and *proboscipedia* transform haltere to wing, antenna-to-leg, and mouthpart-to-leg, respectively (Aplin & Kaufman, 1997; Emerald & Cohen, 2004; Starling Emerald & Roy, 1997). However, the precise mechanism by which Hox regulates tissue or cell growth and size is not yet known*Abdominal A* (*abdA*), a member of the bithorax complex in *Drosophila*, is hierarchically expressed in the abdominal region along the

anterior-posterior axis along with other Hox genes (Lewis, 1978). In the *Drosophila* central nervous system (CNS), cells in the abdominal region of the ventral nerve cord (VNC) express AbdA (Bender et al. 1985; Lewis 1978; Sánchez-Herrero et al. 1985). In addition to providing spatial identity to abdominal neuroblasts or neural stem cells (NSCs), AbdA regulates their temporal fate by limiting the time of abdominal NSC proliferation and terminal fate by controlling their removal from the nervous system (Arya et al., 2015; Bello et al., 2003; Prokop et al., 1998). AbdA regulates the apoptotic elimination of abdominal NSCs in two waves, one during embryonic life and another during larval life (Abrams et al., 1993; Peterson et al., 2002; White et al., 1994).

In this study, we found a significant difference in the growth rate of NSCs in different regions of the *Drosophila* larval VNC (Fig. 1K). Abdominal NSCs grow at a slower rate than those in the thoracic region. Our results showed that AbdA regulates the size of abdominal NSCs and keeps them smaller than thoracic NSCs during larval development. The size of a stem cell is a critical factor that determines its ability to enter mitosis and its rate of proliferation (Britton & Edgar, 1998; Chell & Brand, 2010; Truman & Bate, 1988; Yuan et al., 2020). Abdominal NSCs enter mitosis much later in larval life and produce fewer progeny than thoracic NSCs (Truman & Bate, 1988). We showed that AbdA is necessary and can instructively regulate NSC growth. Upon loss of *abdA* expression, abdominal NSCs grow as large as thoracic NSCs and enter mitosis. In contrast, gain of *abdA* in thoracic NSCs can retard their growth and delay their entry into mitosis. We also found that during normal development, AbdA retards the proliferation rate of abdominal NSCs resulting in fewer progeny. Our study highlights the role of the Hox gene *abdA* in CNS development by controlling the growth, mitosis, and proliferation rates of NSCs.

Results

The NSCs in larval *Drosophila* VNC show spatially restricted size heterogeneity

We used the HES1 protein analog Deadpan (Dpn) to mark the NSC nuclei, and membrane GFP driven with an NSC-specific Gal4 driver inscutable (*insc*) (*insc>mCD8-GFP*) to mark the NSC cell membrane. In the VNC of different larval stages, we noted that the nuclei of abdominal NSCs were smaller than those in the thoracic region (fig. 1A-G'). Since the size of the nucleus is generally proportional to the cytoplasmic volume across different cell types, we checked the cell size of NSCs as well. We also observed the same heterogeneity in cell size when the membrane of each NSC was stained with GFP (fig. 1A-G,I,J). To understand the time at which size differences arose, we profiled the growth patterns of NSCs in the VNC at different embryonic and larval time points. The NSCs in the embryonic VNC were similar in their overall size distribution before entering the quiescence phase and maintained a mean thoracic to abdominal size ratio of one (Fig. 1I,J; Supplementary Fig. 1A, Fig. 2C). During the larval stage, thoracic and abdominal NSCs differentially increased in size and maintained a ratio with a mean value of approximately 1.5, during larval stage 2 (L2), early larval stage 3 (early L3), and mid-larval stage 3 (Mid L3) (Fig. 1I,J; Supplementary Fig. 2C). This indicates that the thoracic NSCs were larger than the abdominal NSCs during all larval stages. The size difference between abdominal and thoracic NSCs at late larval stage 3 (LL3) could not be ascertained because at this stage, all abdominal NSCs were eliminated by apoptosis (Fig. 1H-H'). Size heterogeneity between thoracic and abdominal NSCs has been described previously (Truman and Bate, 1988). Here, we report the detailed growth patterns of these two subtypes during development.

Hox gene *abdA* regulates the growth of abdominal NSCs

To understand whether spatial transcription factors regulate the growth of NSCs, we examined the role of the Hox gene *abdA*, which shows restricted expression in the central abdominal region of the VNC (Lewis, 1978; Sánchez-Herrero et al., 1985, Supplementary Fig. 2A). AbdA regulates the spatial identity of the abdominal VNC region and is expressed in several neural cells beginning at the embryonic stage (Arya et al., 2015; Bender et al., 1985; Lewis, 1978; Prokop et al., 1998; Sánchez-Herrero et al., 1985). Basal expression of AbdA in NSCs can be seen during stage 10-11 embryos, and it is also required for their timely elimination by apoptosis during late embryonic life (Arya et al., 2015; Prokop et al., 1998). Temporal induction of AbdA during late larval life correlates with the removal of the remaining abdominal NSCs through apoptosis (Bello et al., 2003). To understand the role of abdA in the regulation of NSC growth, we knocked down *abdA* using RNAi in NSCs beginning in the embryo. We assessed NSC survival at different larval stages, using the membrane maker mcd8-GFP (*insc>mCD8GF,abdA-RNAi*). Upon knockdown of *abdA*, the number of abdominal NSCs significantly increased at larval stage L2, due to inhibition of apoptosis in the embryo as reported previously (Arya et al., 2015). The overall size distribution was similar to that of the controls (Fig. 2A,B,I,J). However, by early L3, a clear difference in the size of abdominal NSCs was visible in *abdA*-knockdown VNC. *abdA*-depleted NSCs were larger than those in the control (Fig. 2C-H,I,J). We observed a steady increase in the size of *abdA*-depleted abdominal NSCs from stages L2 to LL3 (Fig. 2I,J). Since AbdA expression is limited to the central abdomen, the size of the thoracic NSCs remained unaffected (Supplementary Fig. 2B).

We also noted that on *abdA* knockdown, the size difference between thoracic and abdominal NSCs was reduced. We compared the size of abdominal NSCs with thoracic NSCs in the control and *abdA-knockdown* groups. In early L3, the difference between thoracic and abdominal NSCs was reduced upon *abdA* knockdown compared with that in the control group (Fig. 2K; Supplementary Fig. 2C). Likewise, during Mid L3, unlike the abdominal NSCs, which were approximately 1.6 times smaller than the thoracic NSCs in the control, in VNCs upon *abdA* knockdown, the abdominal NSCs achieved the size of thoracic NSCs (Fig. 2K, Supplementary Fig. 2C). Finally, in LL3, where no abdominal NSCs survived in the control abdominal region, the rescued NSCs in the *abdA* knockdown were as large as the thoracic

NSCs (Fig. 2K, Supplementary Fig. 2C). Thus, AbdA expression in abdominal NSCs appears to regulate their growth pattern.

It has been reported that AbdA is expressed in abdominal NSCs as a pulse between 64-72 hr after larval hatching (ALH) to initiate apoptosis (Bello et al., 2003). Since our results indicated a significant effect of AbdA on the growth of abdominal NSCs beginning with the early larval stage, we undertook a detailed description of the expression pattern of AbdA in the NSCs during the larval period from L1 to L3 (68-70 hr ALH), before the time of abdominal NSCs death (fig. 2L-N'). We used a MiMIC line of *Dpn-GFP*, in which endogenous Dpn protein was tagged with GFP (Nagarkar-Jaiswal et al., 2015). During the very early larval stage (14-17 hr ALH), Dpn-GFP was not detectable in any of the thoracic NSCs. Abdominal NSCs also showed low or no Dpn expression during this stage. AbdA showed widespread differential expression in many cells in the abdominal region, with some cells expressing more AbdA than others (Supplementary fig. 2A). The Dpn-GFP-marked abdominal NSCs showed weak but distinct AbdA expression compared to other cells in this region (fig.2L-N''at early L2 (28-32 hr ALH), early L3 (42-48 hr ALH), and Mid L3 (66-70 hr ALH) stages (Fig. 2L-N').

We also examined the expression of Antennapedia (Antp) and Ultrabithorax (Ubx) proteins in NSCs. They are expressed in the anterior and posterior thoracic region of VNC. We found that Antp was also weakly expressed in NSCs, and. Ubx expression was very low in NSCs (Supplementary Fig. 2G-H'). To further validate the expression of Hox genes in NSCs, we analyzed available single-cell RNA sequencing (scRNA-seq) data (Corrales et al., 2022). Corrales et al. (2022) have sequenced single cells from larval CNS at various developmental time points (1 hr, 24 hr, and 48 hr ALH). We first identified NSCs expressing known markers such as *grh, mira, dpn, CycE, wor, ase,* and *insc* and clustered them using the standard Seurat package (Supplementary Fig. 2D,E,F). Several cells within the cluster were positive for the four Hox genes. In the NSC cluster of larval VNC from different developmental time points, our analysis revealed consistent expression of *Antp*, *AbdA*, and *AbdB* in several cells (Fig. 2O-Q, and Supplementary Fig. 2D-F). *Ubx* was also expressed in several NSCs at 1 hr, but the number was reduced at 48 h ALH.

The difference between our data and previous reports on AbdA expression (Bello et al., 2003; Prokop et al., 1998) could be due to the sensitivity of the analysis. As the expression of Hox genes in NSCs is lower than in other cells, as seen in immunostaining and scRNA-seq data, it

may have been difficult to detect. The presence of Hox genes in NSCs implies a possible post-embryonic role in these cells. As elevated levels of AbdA are known to eliminate NSCs by inducing apoptosis, our data suggest that the continued low expression of AbdA in abdominal NSCs from the early larval stage regulates NSC growth throughout larval life.

The canonical apoptotic pathway does not control the growth of abdominal NSCs

During development, abdominal NSCs are eliminated via apoptosis (Arya et al., 2015; Bello et al., 2003; White et al., 1994). The cell death program begins during the late embryonic stage, dramatically reducing the number of abdominal NSCs (Abrams et al., 1993; Arya et al., 2015a; Peterson et al., 2002; White et al., 1994). The three surviving abdominal NSCs per larval VNC hemi-segment, vm (ventro-medial, 5-2), vl (5-3 ventro-lateral), and dl (dorso-lateral, 3-5), undergo apoptotic elimination at approximately 72 hr ALH (Bello et al., 2003). Thus, despite the presence of several NSCs in the thoracic VNC, the late abdominal VNC is devoid of NSCs. It is important to note that the Hox gene *abdA* is required for NSC apoptosis in both embryonic and larval stages (Arya et al., 2015; Bello et al., 2003).

Loss of cell volume or cell shrinkage is a characteristic of apoptotic cell death. In the *Drosophila* CNS, mushroom body NSCs in the central brain also show retarded growth and a reduction in size before their elimination by apoptosis and autophagy (Siegrist et al., 2010). Thus, we hypothesized that the reduction in NSC size could be linked to cell death pathway activation. To determine whether apoptotic players regulate abdominal NSC size, we blocked apoptosis using different members of the cell death pathway in the hierarchy (Fig. 3A). First, we examined the role of *rpr*, *hid*, and *grim* genes, the most upstream activators of apoptotic signaling, which are transcriptionally activated by death signals (Peterson et al., 2002; White et al., 1994), in regulating abdominal NSC size. To deplete *reaper*, *hid*, and *grim* expression in neural stem cells, we used a microRNA (*UAS-RHG-miRNA*) (Siegrist et al., 2010) that targets all three apoptotic genes. Reduction in the expression of these cell death activators in NSCs (*insc>mCD8GFP;RHG-miRNA*) permitted the continuous survival of abdominal NSCs until the third instar stage due to a failure to undergo apoptosis (Tan et al., 2011). Significantly, the rescued abdominal NSCs were as small as the wild type in the Mid L3 larvae (Fig. 3B,C, E). To further confirm these results, we used homozygous deletion of the MM3 regulatory

genomic region, which controls the expression of the reaper, grim, and sickle pro-apoptotic genes (Tan et al., 2011) (Fig. 3A). InClick or tap here to enter text. agreement with the above results, deletion of the MM3 regulatory region resulted in the survival of abdominal NSCs until the late larval stages. However, their nuclei were as small as in wild-type Mid L3 larvae (Supplementary Fig. 3 A,B).

Finally, we examined the effect of targeted inhibition of active caspases, the downstream effectors of the apoptotic pathway, on the regulation of NSC size. Targeted expression of P35, a promiscuous caspase inhibitor (Fisher et al., 1999), in NSCs (*insc>mCD8GFP;P35*) rescued abdominal NSCs from apoptosis, as previously reported (Bello et al., 2003). Interestingly, the surviving abdominal NSCs were also smaller than the thoracic NSCs (Fig. 3B,D,E). Taken together, our data showed that apoptotic signaling does not regulate the growth of abdominal NSCs.

AbdA regulates the timely entry of abdominal NSCs into mitosis and retards their cycling rate

Proper regulation of the rate and duration of NSC proliferation is essential for maintaining CNS volume, shape, and function. We found that AbdA controls the growth of abdominal NSCs and keeps them smaller than the thoracic NSCs. It is important to note that although the thoracic and abdominal cells enter into the S phase at approximately 30 hr ALH, the abdominal NSCs become mitotically active much later, at approximately 50hr ALH (Truman & Bate, 1988, Taylor and Truman 1992). Since abdominal NSCs also proliferate slower than thoracic NSCs (Truman & Bate, 1988, Fig. 4A), we investigated whether the late entry of abdominal NSCs into mitosis is regulated by *abdA*. Upon *abdA* knockdown, several abdominal NSCs in Mid L3 produced larger numbers of progeny than the control of the same age (Fig. 2 E,F). For a NSC to produce a bigger lineage, either the duration of its proliferation could be longer, or proliferation could be faster. Since the rescued abdominal NSCs in the *abdA* knockdown were larger, we first checked their mitotic entry window. Usually, abdominal NSCs enter mitosis at approximately 55 hr ALH (Truman & Bate, 1988, Fig. 4A). However, upon *abdA* knockdown, NSCs began to divide much earlier. When checked at 48-52 hr ALH, they have already produced 2-6 progeny (Fig. 4A,D). To ensure that the progeny present here were not born embryonically, we checked an earlier window of 21 to 26 hr in *abdA* knockdown and found no proliferation at this stage

(Fig. 2B), indicating that abdominal NSCs became mitotically active between Mid of L2 and before onset of Early L3. Since rescuing apoptosis by expressing P35 does not affect the abdominal NSC mitotic window, we conclude that the inhibition of cell death alone is not responsible for this early mitotic entry (Fig. 4 compares C and D). We evaluated the size of abdominal NSCs in control, P35, and *abdA* knockdown conditions at 48-52 hr ALH. The abdominal NSCs in the *abdA*-knockdown VNC were approximately 1.3 times bigger than the control and P35 expressing cells (Fig. 4E). Therefore, we propose that the increase in abdominal NSC size could be responsible for early entry into mitosis after *abdA* loss.

Thoracic NSCs divide faster than abdominal NSCs (Truman and Bate, 1988). In general, thoracic NSCs divide in 55 min compared to abdominal NSCs, which take more than 2 hrs to complete one cell division (Truman & Bate, 1988). To determine whether AbdA also affects the rate of cell cycle progression, we used EdU incorporation. We administered a one-hr EdU pulse to the mid L3 (65-73 hr ALH), which is the active proliferative window of abdominal NSCs (Fig. 4A) and compared EdU incorporation into NSCs and their progeny in the control and experimental groups. Significantly more EdU+ NSCs and GMCs were observed on the ventral side of the VNC upon *abdA* knockdown than in the control. Similarly, NSCs in the ventrolateral and dorsolateral regions of the abdominal region of the VNC also incorporated more EdU upon *abdA* knockdown than did those in the control (fig. 4F). The data indicate that abdAslows the cell division rate of abdominal NSCs.

AbdA is sufficient to restrict the growth of thoracic NSCs and delay their entry into mitosis

We showed that AbdA restricted the growth of abdominal NSCs. To further check whether AbdA is sufficient to regulate the growth of NSCs, we investigated whether its ectopic expression could also restrict the growth of thoracic NSCs. We expressed *abdA* in NSCs from embryonic life (*insc>mCD8GFP,abdA*) and evaluated thoracic NSCs size. It is important to note that ectopic expression of Hox genes, including *abdA*, induces apoptosis of NSCs (Bello et al., 2003). To study the role of *abdA* in growth regulation, we inhibited NSC apoptosis by co-expressing the caspase inhibitor, P35 (*insc>mCD8GFP,abdA;P35*). Interestingly, ectopic expression of *abdA* restricted the growth of thoracic NSCs in the LL3 (Fig. 5A-D, I). In the

control, the size of thoracic NSCs was in the range of 8-14 um, and upon expression of *abdA*, it reduced to 5-12 um, which is 1.2 times smaller than the ones present in the control in the LL3 CNS (Fig. 5I). We noted that thoracic NSCs expressing *abdA* also showed growth retardation over time (Fig. 5K,L). We inferred that AbdA could instruct the growth retardation program in NSCs.

Since ectopic expression of *abdA* reduced the size of thoracic NSCs, we investigated whether these small-sized NSCs entered mitosis at the right time. Normally, thoracic NSCs exit quiescence at 28-30 hr ALH (Truman & Bate, 1988)((Fig. 5M). We found that ectopic expression of *abdA* not only restricted NSCs growth, but also delayed their entry into mitosis, and they remained non-dividing at 31-35 hr ALH (Fig 5. E-H,J-M). We also expressed *P35* with *abdA* as a control to nullify the apoptosis-inducing role of *abdA* in NSCs (Fig. 5G, H). Taken together, we conclude that *abdA* regulates the timing of NSC entry into mitosis and NSC growth. The two effects are strongly correlated but could reflect independent activities of *abdA*.

AbdA loss is insufficient to initiate the growth of NSCs on nutrient deprivation

Several studies have shown that the nutritional signal-dependent growth of NSCs is necessary for their entry into mitosis (Britton & Edgar, 1998; Chell & Brand, 2010; Yuan et al., 2020). When larvae start actively feeding, the presence of circulating dietary amino acids in the hemolymph is detected by fat bodies, which secrete fat-body-derived mitogens (FBDM) into the hemolymph (Britton & Edgar, 1998). FBDM then stimulates surface glia to secrete dILPs (*Drosophila* insulin-like peptides), which activate NSCs growth via dlnR/PI3K/Akt signaling (Chell & Brand, 2010; Sousa-Nunes et al., 2011). Under nutrition-restricted conditions, the thoracic NSCs of larvae neither grow nor enter the cell cycle (Britton & Edgar, 1998; Chell & Brand, 2010; Yuan et al., 2020).

Notably, a small group of NSCs, such as the mushroom body and lateral NSCs in the *Drosophila* brain, do not depend on nutrition for proliferation. These cells grow and proliferate early during larval life, even without nutrition (Britton & Edgar, 1998; Truman & Bate, 1988; Yuan et al., 2020). We asked if the loss of AbdA makes the abdominal NSCs grow independent of nutrient availability. Does an early increase in the growth of these cells upon

abdA loss occur in the absence of nutritional signals? To analyze the relationship between nutrition and AbdA on the growth of abdominal NSCs, we selected two developmental time points during larval life: one at which the abdominal NSCs started mitosis (approximately 50 hr ALH) and another when most of them actively engaged in proliferation (approximately 65 hr ALH) (Fig. 6J). Under nutrition-restricted conditions, neither thoracic nor abdominal NSCs grew or entered the cell cycle in the control group, as reported earlier (Britton and Edgar, 1998; Chell and Brand, 2010; Yuan et al., 2020) (Fig. 6D-E,G-J). Similarly, abdA-downregulated abdominal NSCs did not increase in size or enter mitosis even at 65 hr ALH (fig. 6F-J). We compared the size of Mid L3 NSCs (65-68 hr ALH) in the sucrose-fed yeast deprived control group and *abdA*-knockdown animals and found that in both cases, the sizes of thoracic and abdominal NSCs were smaller than those in the amino acid-fed larvae and they also did not enter mitosis (fig. 6A-H). These smaller NSCs also have a tail-like projection found in quiescent NSCs (Truman & Bate, 1988, arrow in fig. 6D-F). Our findings indicate that size-related control of AbdA acts downstream of nutritional signaling when NSCs become competent for growth. We concluded that nutritional signals are responsible for the growth and cell cycle entry of NSCs and that AbdA in abdominal NSCs retards their growth and proliferative potential once they resume growth.

Discussion:

Growth of NSCs is essential to realize their full potential

Our study identified the functional significance of NSC heterogenous growth in determining their spatial and temporal fate in the developing *Drosophila* CNS.Click or tap here to enter text. Since diverse sets of neurons in precise numbers innervate different body parts, neuron formation is a tightly regulated developmental event (Doe & Technau, 1993; Hartenstein & Campos-Ortega, 1984; Truman & Bate, 1988). Immediately after NSCs are born in the embryonic CNS, they divide to produce neurons and glial cells (Ito et al., 2013; Knoblich, 2008; li Ming & Song, 2011; Schmidt et al., 1997; Yu et al., 2013). Although all NSCs in different hemi-segments of the developing embryonic CNS share a common identity, their fate is regulated by their spatial location in the CNS (Sen et al., 2019). By the end of embryonic life, most surviving NSCs in the VNC become smaller and enter quiescence (Hartenstein et al.,

1987). These quiescent NSCs again increase their size during larval life and resume the cell cycle to produce neurons in adult flies (Truman & Bate, 1988).

It is important to note that NSCs in the brain and thoracic region of the VNC produce neurons into the pupal stages, whereas abdominal NSCs generate neurons only until larval stage (Bello et al., 2003; Truman & Bate, 1988). Notably, NSC size is closely correlated with exit from quiescence and may determine the timing of exit and the duration of proliferation during the life of NSCs. The thoracic NSCs in the VNC gradually decrease in size during pupal life before undergoing symmetric division to form two terminally differentiated cells (Homem et al., 2014;). Similarly, mushroom body NSCs in the fly brain also reduce size before autophagy and apoptosis are eliminated (Siegrist et al., 2010). We found that abdominal NSCs are the smallest of all types of NSCs present in the *Drosophila* CNS, and that the *abdA* Hox gene regulates their growth (Figure 7 model). The growth rate of these cells is very slow; they enter mitosis late, cycle slowly, and produce a smaller number of progeny. We noted that the expression of AbdA in all abdominal NSCs from the early larval stage slows their growth and delays their entry into mitosis compared to thoracic NSCs. This is one of the reasons why these cells produce fewer progeny. Another reason why abdominal NSCs produce fewer progeny is their slow cycling rate (Truman and Bate, 1988). Interestingly, when thoracic NSCs complete one cycle of cell division in less than an hour, abdominal NSCs take twice as long (Truman & Bate, 1988). We observed that AbdA plays a crucial role in regulating the cell cycle rate of NSCs. The continued presence of AbdA in these cells does not allow them to grow as large as their thoracic neighbors; and, they cycle slowly and produce fewer progeny. The size of a stem cell may be crucial in determining the appropriate time to give birth to neurons and determining how many neurons to be born to innervate a specific tissue.

The regulation of NSC growth and mitotic entry involves a complex interplay of signaling pathways, including insulin, PI3K/Akt/TOR, and Hippo. Insulin signaling plays a vital role in breaking the quiescent state of most type I NSCs (Britton & Edgar, 1998; Chell & Brand, 2010; Ding et al., 2016; Sousa-Nunes et al., 2011). With the availability of circulating amino acids in the nervous system, the PI3K/Akt/TOR pathways become active, removing inhibitory Hippo signaling to initiate NSC growth (Britton & Edgar, 1998; Chell & Brand, 2010; Ding et al., 2016; Sousa-Nunes et al., 2011). Thus, these growth pathways tightly control the switch between the nondividing state and the proliferative state of NSCs The availability of

nutrients makes NSCs competent for growth and entry into mitosis. We noted that the growth retardation signal of AbdA only functions when NSCs achieve competence to grow in the presence of a nutritional signal. In a nutrition-deprived state, *abdA* knockdown failed to initiate the growth of abdominal NSCs, indicating that *abdA* acts downstream of nutrition to fine-tune the growth rate of abdominal NSCs. These findings suggest that nutritional signals are responsible for initiating the growth of all type I NSCs and that the presence of AbdA in abdominal NSCs acts as a growth retardation signal to maintain their growth. This specific role of *abdA* in NSC growth regulation provides a deeper understanding of the complex mechanisms involved in the regulation of the fate of NSCs.

The Hox gene *abdA* is an important fate determinant of abdominal NSCs

During development, Hox genes, including *abdA*, play crucial roles as regulators of specific signaling pathways. They operate in a tissue-specific manner to determine the correct body patterning, including tissue formation at an appropriate location. (Lewis, 1978; Mann & Morata, 2000; Marin et al., 2012; Miller et al., 2001; Rogulja-Ortmann & Technau, 2008). In the *Drosophila* nervous system, AbdA is a significant determinant of spatiotemporal fate. It is expressed in the central abdominal region of embryonic and larval nervous system (Arya et al., 2015; Lewis, 1978; Sánchez-Herrero et al., 1985). *abdA* is well known for its role in regulating the apoptosis of abdominal NSCs during embryonic and larval life via the canonical cell death pathway (Arya et al., 2015; Bello et al., 2003;). Previously, it was shown that larval abdominal NSCs do not express AbdA, and only act as a pulse at a specific time to induce apoptotic signaling (Bello et al. 2003). It has been suggested that Hox genes in NSCs might create a stable memory imprint during their early expression in embryonic life, which stably regulates the fate of NSCs even in their absence (Prokop et al., 1998). In contrast, our study revealed that NSCs express *abdA* and other Hox genes, such as *Antp* and *Ubx*, from the very early larval stage, although their expression levels are low. The expression of AbdA helps control the growth of these cells, regulating their entry into mitosis and their potential for proliferation.

To form a functional CNS, tissue growth is coordinated at multiple levels. In this study, we found that AbdA regulates the growth of NSCs, and determines their potential to form neurons. In *Drosophila*, post-embryonic NSCs in the larval CNS regain their activity and enter the cell

cycle to develop into functional adult CNS. It is intriguing that not all NSCs in the CNS start proliferating simultaneously. Instead, they follow a temporal pattern along the anterior-posterior axis to enter mitosis (Truman and Bate, 1988). At approximately 30 h ALH, the thoracic NSCs entered S phase and started proliferating. It is important to note that the abdominal NSCs enter into S phase at the same time as thoracic NSCs, but they start proliferation 20 hr later, at approximately 50 hr ALH (Truman and Bate, 1988, Taylor and Truman 1992). Therefore, it is important to understand the factors that delay the entry of NSCs into mitosis. Our data strongly suggest that the slow growth of these cells due to AbdA expression does not allow them to become mitotically active earlier and divide as fast as their thoracic neighbors.

Conclusion

Our study highlights an important role of hox gene AbdA in regulating abdominal NSCs growth and determining their mitotic potential. From the onset of larval life and the availability of nutrition, both thoracic and abdominal NSCs resume growth and gradually enter mitosis. During larval development, we observed that both the thoracic and abdominal NSCs grew in size. However, the rate of abdominal NSC growth is always slower than that of thoracic NSC; thus, they always remain smaller than the thoracic NSCs. We noted that *abdA* regulates the rate of abdominal NSC growth. We suggest that *abdA* retards the growth of abdominal NSCs and regulates their potential to generate only a limited number of neurons in the correct temporal window. Loss of *abdA* expression in NSCs allows them to grow faster, enter mitosis earlier, and initiate neurogenesis in an ectopic window, which may adversely affect the normal development of an organism. Thus, *abdA* may retard the growth of abdominal NSCs to prolong the non-dividing period and control neurogenesis in this region, both spatially and temporally. *abdA* also regulates the timely removal of these NSCs from the nervous system. This finding has significant implications for our understanding of neurogenesis as it provides insights into the regulatory mechanisms that control the timing and extent of NSC growth for subsequent neurogenesis.

Materials and Methods

Fly stocks

Drosophila melanogaster was reared at 25ºC ±1and crosses were performed at 25 °C in an incubator on a standard food medium containing sugar, agar, maize powder, and yeast. Appropriate fly crosses were set up following standard method to obtain the progeny of desired genotypes (Yadav et al., 2024). The following fly stocks were used in the experiment: wild-type Oregon R +, *inscutable-Gal4,* also known as *1407-Gal4* (a generous gift from Dr. J. A. Knoblich, Vienna, Austria) recombined with UAS-mCD8GFP (BL-5137), *abdA-RNAi* (BL-35644, v106155), *Dpn-GFP* (BL-59755) *UAS-P35* (BL-5073), *UAS-abdA* (BL-912), *UAS-P35* (BL-5073).

Immunostaining, confocal microscopy, and documentation

Larvae F1 progeny of different ages from L1 (17-18 hr ALH), L2 (21-26 hr ALH) , Early L3 (48-52 hr), Mid L3 (66-73 hr) and Late L3 (LL3, 80-84 hr ALH) obtained from set crosses of specific genotypes, larvae were selected by choosing GFP reporter and CNSs were dissected in Phosphate buffer solution (PBS 1X containing NaCl, KCl, Na2HPO4, KH2PO4, pH-7.4), fixed in 4% Paraformaldehyde for 30 min., rinsed in 0.1% PBST, (1X PBS , 0.1% Triton X-100), then added in blocking solution (0.1% Triton X-100, 0.1% BSA, 10% FSC, 0.1% deoxycholate, 0.02% Thiomersol) for 1 hr at room temperature. The tissues were incubated with the following primary antibodies: rat anti-Dpn (1:150,195173 and abcam), chicken anti-GFP (1:1000,A10262, Invitrogen), and kept at 4°C for two consecutive overnight incubations, anti-abdA (c-11) (sc-390990, Santa Cruz). The following day, tissues were rinsed thrice with 0.1% PBST (15 min each), incubated with 1 a200 dilution of appropriate secondary antibodies, anti-rat 546 (A11081 and Alexa Fluor, Invitrogen), anti-chicken 488 (A11039 and Alexa Fluor, Invitrogen), and anti-mouse 647 (A21235 and Alexa Fluor, Invitrogen) overnight at 4 °C, and incubated for 2 h at room temperature. Following incubation with secondary antibodies, the samples were washed three times with 0.1% PBST and mounted with DABCO (D27802; Sigma-Aldrich) for further analyses.

Images were acquired using a Leica SP8 STED confocal microscopy facility at the CDC, BHU,India and Zeiss LSM-510 meta, Department of Zoology BHU, India, Nikon A1SiR confocal at MGH USA, Images were assembled using Adobe Photoshop and MS PowerPoint.

EdU labeling:

The 5-ethynyl-2'-deoxyuridine (EdU) assay was performed using a click it-488 (C10337 and Click-it, Invitrogen) by soaking the dissected CNS for 1 hr. After soaking, the CNS were fixed for 20 min in 4% formaldehyde, washed twice with 3% BSA in PBS, and permeabilized with 0.5% Triton X-100 in PBS twice for 20 min. Incorporated EdU was detected by Click-iT fluorescent dye azide reaction in accordance with the manufacturer's instructions protocol given in the kit.

Image analysis using Fiji and Graph Pad prism

All images were quantified using the Fiji/Image J software (NIH, USA). To measure the NSC size, a freehand tool was used to mark the length and width of the NSC. As the NSC shape was not fully round, two perpendicular lines were drawn along the center of the NSC at its widest point, and their average was considered to be the NSC diameter. Size was measured using the analysis measure option in Fiji.

Graphs were created using GraphPad Prism9 and Ms Excel. Statistical analysis was performed using GraphPad Prism9, where two-tailed unpaired t-tests were used to evaluate statistic<0.05(****P<0.0001, ***P<0.001, **P<0.01, *P<0.05) considered statistically significant, and P>0.05 considered nonsignificant.

Violon plots were constructed using the GraphPad Prism9. The spread of NSC diameter is shown from the median and quartile ranges of distribution in individual groups.

Nutritional regimen

Control groups were fed a standard *Drosophila* diet of maize, agar, sucrose, yeast, and propionic acid. Starved larvae were yeast-deprived and fed the standard diet components mentioned above; sucrose concentrations were 20% in the diet (Britton & Edgar, 1998). An extra sucrose containing 1x PBS solution-soaked cotton was also given to the larvae. After hatching the larvae from the embryo, they were transferred to yeast-free food media.

Single cell RNA sequencing (scRNA-Seq) analysis

Processed scRNA data sets (Seurat files) at 1 hr, 24 hr, and 48 hr after larval hatching (ALH) were obtained from published data sets (Corrales et al 2022). Matrix, barcode, and feature files

were downloaded from GEO (GSE135810). five samples were used - GSM 4030601, GSM 4030603, GSM 4030605, GSM 4030613 and GSM 4030614. All analyses were performed using the Seurat R package version 5.1.0. Samples corresponding to the same time point were merged to create three unified seurat objects corresponding to each time point.

Low quality cells (less than 200 features, less than 10% ribosomal RNA and more than 10 % mitochondrial RNA) were not included in the analyses for each Seurat object. Reads for mitochondrial and ribosomal genes were excluded. Principal Component analysis was done using the top 3000 highly variant features. Elbow plot was computed to decide the number of Principal Components (PCs) to be used for downstream analysis. We used the first 30 PCs to cluster the cells using the default Louvain algorithm. The default resolution was used to cluster the cells. 8331, 7657, and 6380 cells were obtained at 1 hr, 24 hr, and 48 hr, respectively. Clusters were identified using known markers as described by Dillon et al. 2022. The expression of four Hox genes known to be expressed in VNC, *Antp, Ubx, abdA*, and *AbdB* was studied in these clusters.

Figure legends

Figure 1. NSCs in *Drosophila* VNC exhibit a spatially restricted size heterogeneity. (A-D) thoracic NSCs (A'-D') are magnified areas of the same images. (E-H) NSCs in abdominal NSCs (E'-H') magnified areas of the same images. In all images, NSC nuclei marked by Deadpan (red) and mCD8GFP (green) mark the membrane of NSCs and their progeny (*insc>UAS-mCD8GFP*). (I) Graphically depicts NSC size in the thoracic and abdominal regions during different developmental stages. "X" in the graph indicates apoptosis of NSCs. The violin plot shows the overall distribution of the NSC size for different VNCs. (J) shows how thoracic and abdominal NSCs gradually increase in size during different developmental stages; error bars show standard error in size difference. (K) A model depicting *Drosophila* CNS with brain and VNC, showing type 1 NSCs (red circles) and bigger Mushroom body NSCs (blue circles). Statistical evaluation of significance based on an unpaired t-test is marked with asterisks; ****P<0.0001. Scale bar: 20 µm and 5 µm for magnified images. More than five CNS cases were analyzed for each case.

Figure 2. *abdA* restricts growth of abdominal NSCs. (A–H) Abdominal NSCs increased in size over the larval stages (from L2 to LL3) in the control group (A, C, E, *insc>mCD8GP*). The control in (G) shows no NSC. (B,D,F,H) *abdA* knockdown (*insc>mCD8GP;abdA-RNAi*) results in a more pronounced increase in NSCs size at different larval stages. (I-J) Graph showing the growth of abdominal NSCs in control and *abdA* knockdown from L2 to Late L3 stages. (K) Violin plots showing that NSC size differences between thoracic and abdominal NSCs became narrower upon abdA knockdown. "X" indicates developmental loss of NSCs in

late L3 due to apoptosis. (L-N) Single sections of confocal images showing AbdA expression in abdominal NSCs (white arrow) during different larval stages. (O-Q) Bar plots of scRNA-Seq showing the number of NSCs that express the four Hox genes, Antp, Ubx, AbdA and AbdB in the larval VNC at 1 hr, 24 hr, 48 hr ALH, respectively. An expression threshold (E) > = 0.5 is considered positive. The expression threshold was set for logarithm-normalized expression levels. ALH After Larval Hatching. Statistical evaluation of significance based on an unpaired t-test is marked with asterisks; ****P<0.0001. Scale bar: 20 µm. More than five CNS cases were analyzed in each case.

Figure 3. The canonical cell death pathway does not regulate the size of the abdominal NSCs. (A) A model depicting abdominal NSCs apoptotic regulation by abdA. (B-D) Size of nuclei of NSCs in the abdominal region in control mid L3 (*insc>mCD8GFP*) and Late L3 of RHGmiRNA (*insc>mCD8GFP,RHGmiRNA*) and P35 (*insc>mCD8GFP;P35*) appeared to be of the same size. The insets show a magnified view of the NSCs marked with Dpn and mCD8GFP. (E) Quantification of the size of surviving abdominal NSCs in all genotypes shown in (B-D) was similar, with no significant difference. The statistical evaluation of significance based on an unpaired t-test is marked with asterisks, ****P<0.0001. Scale bar: 20 µm. More than 5 CNS were analyzed in each case.

Figure 4. AbdA regulates the timely entry of abdominal NSCs into mitosis and retards their cycle rate. (A) Schematic showing the duration of active cycling of thoracic and abdominal NSCs, lines depicting the active proliferation window, and arrow showing the shift of the NSC proliferation window earlier. (A-D) 48-52ALH abdominal NSCs in control (B,C *insc>mCD8GFP* and *insc>mCD8GFP;P35*) were quiescent and did not produce progeny, whereas in abdA-knockdown VNC (D, *insc>mCD8GFP; abdA-RNAi*), NSCs entered mitosis and formed progeny; insets show NSCs marked with Dpn and mCD8GFP. (E) Quantification of the NSC size for the datasets shown in A-D. (F) Graph showing the counts of EdU+ NSCs and GMCs in various combinations, upon 1 hr EdU pulse at 69 to 73 hr ALH , (‘‘+’’, ‘‘-’’ indicate EdU positive and negative cells respectively) showing that more NSCs and GMCs incorporate EdU upon *abdA* knockdown. The statistical evaluation of significance based on an unpaired t-test is marked with asterisks, ****P<0.0001. Scale bar: 20 µm. More than 5 CNS were analyzed in each case.

Figure 5. *AbdA* is sufficient to restrict the growth of thoracic NSCs and delay their entry into mitosis. (A-D) NSC size reduction upon ectopic abdA expression in Late L3 larvae. Thoracic NSCs in (A,B) controls (*insc>mCD8GFP, insc>mCD8GF;P35*), and (C,D) ectopic AbdA expression (*insc>mCD8GFP,abdA, and Insc>mCD8GFP,abdA;P35*). Note that the NSCs are smaller in C and D compared to A and B. (E-H) Small NSCs expressing ectopic abdA did not enter mitosis at the designated time. Thoracic NSCs during 30-35 hr ALH in (E, F) control (*insc*>mCD8GFP, *insc>mCD8GFP;P35*) already have proliferating NSCs, as shown in the inset with GFP positive lineage, whereas in (G,H) upon ectopic AbdA expression (*insc>mCD8GFP,abdA and insc>mCD8GFP,abdA;P35*), the NSCs do not have lineage around (inset). (I,J) Quantification of data presented in A-D and E-H. (K, L) Quantification of the growth pattern of thoracic NSCs upon ectopic abdA expression at different developmental stages showing apparent retardation in growth. (M) The summary schematic shows the delay in mitotic entry upon abdA ectopic expression compared to the control; the arrow

shows a shift in the NSC proliferation window later. The statistical evaluation of significance based on an unpaired t-test is marked with asterisks, ****P<0.0001. Scale bar: 20 µm. More than 5 CNS were analyzed in each case.

Figure 6. AbdA loss is insufficient to initiate the growth of Starved NSCs. (A-C) Well-fed larvae at 65-68 hr ALH thoracic and abdominal NSCs in (A,B) control (*insc>mCD8GFP, insc>mCD8GFP; P35*) and (C) abdA-knockdown (*insc:mCD8GFP>abdA RNAi*) groups showed active proliferation and the presence of GFP-positive progeny cells. (D-F) Under starved conditions, neither controls (D,E) nor NSCs with abdA knockdown (F) showed signs of mitotic entry quiescence exit. Insets show zoomed-in views of the respective genotypes. Arrows in the insets show tail-like projections of the quiescent NSCs. (G-H) Quantification of NSC size data is presented in (A-F). (I,J) Summary diagram showing the active proliferation windows in thoracic and abdominal NSC under fed and starved conditions. The star (*) indicates the time at which we evaluated the non-dividing status of NSCs. The arrow showing the NSC proliferation window shifted earlier in *abdA-knockdown cells*. The statistical evaluation of significance based on an unpaired t-test is marked with asterisks, ****P<0.0001. Scale bar: 20 µm. More than 5 CNS were analyzed in each case.

Figure 7: A model depicting change in size of abdominal NSCs and shift in their proliferation window upon *abdA* knockdown. Control *(insc>mCD8GFP),* abdominal NSCs (red) remain smaller and produce progeny (green) by around 55hr ALH. Upon *abdA* knock down *(insc>mCD8GFP;abdA RNAi),* abdominal NSC grow bigger and enter mitosis earlier, thus produce more progeny than control. Progeny numbers made are schematic representations only.

Supplementary figure 1. (A,B) Stage 15 and 16 embryos showing NSCs (marked by Dpn) in the thoracic and abdominal VNC (dotted line separates thoracic and abdominal VNC). Scale bar: 20 µm.

Supplementary figure 2 (A) abdA-expressing region in abdominal VNC (B) thoracic NSC size in control (*insc>mCD8GFP)* and abdA-knockdown (*insc>mCD8GFP,abdA-RNAi*). (C) Ratio of thoracic vs. abdominal NSC size in control (*insc>mCD8GFP*) and *abdA* knockdown (*insc>mCD8GFP,;abdA-RNAi*). (D-F) Dot plots of marker genes for NSCs at 1 hr, 24 hr and 48 hr. All clusters were identified using markers, as previously described (Dillon et al. 2022). thor and trbl distinguish quiescent NSCs from other cell types. *grh*, *mira*, *dpn*, *CycE*, *wor*, *ase*, and *insc* mainly mark type I NSCs and show low expression in quiescent NSCs (qNSCs) at 1h. The qNSC cluster at 1h consists of 466 cells, at 24 hr, it has 55 cells. The type I NSC cluster at 24 hr had 225 cells, and the 48 hr sample had 46 cells in the NSC cluster. (G-H') Antp and Ubx expression in NSCs. Scale bar: 20 µm.

Supplementary figure 3. (A) Late L3 VNC of the *MM3* deletion line, with both thoracic and abdominal NSCs marked by Dpn. (B) *MM3* does not affect the size of the rescued NSC. The statistical evaluation of significance based on an unpaired t-test is marked with asterisks, ****P<0.0001. Scale bar: 20 µm. N=5.

Acknowledgements

We thank Profs. S. C. Lakhotia, B.C. Mondal, G. K., and Pandey, for critically reviewing the manuscript. We thank the Bloomington *Drosophila* Stock Center (BDSC), NIH P40OD018537, for providing fly stocks and FlyBase release (FB 2022_03) for information on fly genes. We also thank the Cytogenetic Laboratory, Department of Zoology, for all instrumental facilities. We thank Ramkrishna Mishra and Vaishali Yadav for their assistance during the experiments.

Funding

This work was supported by grants from NIH (GM110477) to KW, the Department of Science and Technology, Science and Engineering Research Board (DST-SERB, ECR/2018,/002837, CRG/2022/006350), Government of India New Delhi, Department of Biotechnology (DBT) Ramalingaswami re-entry fellowship(BT/RLF/Re-entry/30/2015) and BHU-IoE to RA, CSIR-University Grants Commission (CSIR-UGC, 20161011929) for providing NET-JRF to PD.

Conflict of interest

The author (s) declare no conflict of interest.

Author contributions

All the authors contributed to the study. The work started in KW lab at MGH, USA. P.D. performed the animal experiments, designed workflow, image acquisition, quantification of acquired data, statistical analysis, and created a figure panel under the supervision of R.A. Data curation and analysis presented in Fig. 2O-Q and Supplementary Fig. 2D-F were done by S. M. and E.A., data visualization was done by E.A.

References

1. Abrams, J. M., White, K., Fessier, L. I., & Steller, H. (1993). Programmed cell death during Drosophila embryogenesis. *Development*, *117*(1), 29–43. https://doi.org/10.1242/dev.117.1.29
2. Aplin, A. C., & Kaufman, T. C. (1997). Homeotic transformation of legs to mouthparts by proboscipedia expression in Drosophila imaginal discs. *Mechanisms of Development*, *62*(1), 51–60. https://doi.org/10.1016/S0925-4773(96)00649-1
3. Arya, R., Sarkissian, T., Tan, Y., & White, K. (2015). Neural stem cell progeny regulate stem cell death in a Notch and Hox dependent manner. *Cell Death and Differentiation*, *22*(8), 1378–1387. https://doi.org/10.1038/cdd.2014.235
4. Bello, B. C., Hirth, F., & Gould, A. P. (2003). A pulse of the Drosophila Hox protein Abdominal-A schedules the end of neural proliferation via neuroblast apoptosis. *Neuron*, *37*(2), 209–219. https://doi.org/10.1016/S0896-6273(02)01181-9
5. Bender, W., Weiffenbach, B., Karch, F., & Peifer, M. (1985). Domains of cis-interaction in the bithorax complex. *Cold Spring Harbor Symposia on Quantitative Biology*, *50*, 173–180. https://doi.org/10.1101/SQB.1985.050.01.023

6. Britton, J. S., & Edgar, B. A. (1998). Environmental control of the cell cycle in Drosophila: nutrition activates mitotic and endoreplicative cells by distinct mechanisms. *Development (Cambridge, England)*, *125*(11), 2149–2158. https://doi.org/10.1242/DEV.125.11.2149
7. Cadart, C., Monnier, S., Grilli, J., Sáez, P. J., Srivastava, N., Attia, R., Terriac, E., Baum, B., Cosentino-Lagomarsino, M., & Piel, M. (2018). Size control in mammalian cells involves modulation of both growth rate and cell cycle duration. *Nature Communications*, *9*(1). https://doi.org/10.1038/s41467-018-05393-0
8. Campos-Ortega, J. A., & Knust, E. (1990). Genetics of early neurogenesis in Drosophila melanogaster. *Annual Review of Genetics*, *24*(1), 387–407. https://doi.org/10.1146/annurev.ge.24.120190.002131
9. Chai, P. C., Liu, Z., Chia, W., & Cai, Y. (2013). Hedgehog Signaling Acts with the Temporal Cascade to Promote Neuroblast Cell Cycle Exit. *PLoS Biology*, *11*(2). https://doi.org/10.1371/journal.pbio.1001494
10. Chell, J. M., & Brand, A. H. (2010). Nutrition-responsive glia control exit of neural stem cells from quiescence. *Cell*, *143*(7), 1161–1173. https://doi.org/10.1016/j.cell.2010.12.007
11. Corrales, M., Cocanougher, B. T., Kohn, A. B., Wittenbach, J. D., Long, X. S., Lemire, A., Cardona, A., Singer, R. H., Moroz, L. L., & Zlatic, M. (2022). A single-cell transcriptomic atlas of complete insect nervous systems across multiple life stages. *Neural Development*, *17*(1). https://doi.org/10.1186/S13064-022-00164-6
12. Ding, R., Weynans, K., Bossing, T., Barros, C. S., & Berger, C. (2016). The Hippo signalling pathway maintains quiescence in Drosophila neural stem cells. *Nature Communications*, *7*. https://doi.org/10.1038/ncomms10510
13. Doe, C. Q. (2017). Temporal patterning in the drosophila CNS. *Annual Review of Cell and Developmental Biology*, *33*(Volume 33, 2017), 219–240. https://doi.org/10.1146/ANNUREV-CELLBIO-111315-125210/CITE/REFWORKS
14. Doe, C. Q., & Technau, G. M. (1993). Identification and cell lineage of individual neural precursors in the Drosophila CNS. *Trends in Neurosciences*, *16*(12), 510–514. https://doi.org/10.1016/0166-2236(93)90195-R
15. Emerald, B. S., & Cohen, S. M. (2004). Spatial and temporal regulation of the homeotic selector gene Antennapedia is required for the establishment of leg identity in Drosophila. *Developmental Biology*, *267*(2), 462–472. https://doi.org/10.1016/j.ydbio.2003.12.006
16. Fisher, A. J., dela Cruz, W., Zoog, S. J., Schneider, C. L., & Friesen, P. D. (1999). Crystal structure of baculovirus P35: Role of a novel reactive site loop in apoptotic caspase inhibition. *EMBO Journal*, *18*(8), 2031–2039. https://doi.org/10.1093/emboj/18.8.2031
17. Ginzberg, M. B., Chang, N., D'souza, H., Patel, N., Kafri, R., & Kirschner, M. W. (2018). Cell size sensing in animal cells coordinates anabolic growth rates and cell cycle progression to maintain cell size uniformity. *ELife*, *7*. https://doi.org/10.7554/eLife.26957
18. Hartenstein, V., & Campos-Ortega, J. A. (1984). Early neurogenesis in wild-type Drosophila melanogaster. *Wilhelm Roux's Archives of Developmental Biology*, *193*(5), 308–325. https://doi.org/10.1007/BF00848159
19. Hartenstein, V., Rudloff, E., & Campos -Ortega, J. A. (1987). The pattern of proliferation of the neuroblasts in the wild-type embryo of Drosophila melanogaster. *Roux's Archives of Developmental Biology*, *196*(8), 473–485. https://doi.org/10.1007/BF00399871/METRICS
20. Homem, C. C. F., Steinmann, V., Burkard, T. R., Jais, A., Esterbauer, H., & Knoblich, J. A. (2014). Ecdysone and mediator change energy metabolism to terminate proliferation in drosophila neural stem cells. *Cell*, *158*(4), 874–888. https://doi.org/10.1016/j.cell.2014.06.024
21. Ito, M., Masuda, N., Shinomiya, K., Endo, K., & Ito, K. (2013). Systematic analysis of neural projections reveals clonal composition of the Drosophila brain. *Current Biology*, *23*(8), 644–655. https://doi.org/10.1016/j.cub.2013.03.015
22. Jacob, J., Maurange, C., & Gould, A. P. (2008). Temporal control of neuronal diversity: common regulatory principles in insects and vertebrates? *Development (Cambridge, England)*, *135*(21), 3481–3489. https://doi.org/10.1242/DEV.016931
23. Kafri, R., Levy, J., Ginzberg, M. B., Oh, S., Lahav, G., & Kirschner, M. W. (2013). Dynamics extracted from fixed cells reveal feedback linking cell growth to cell cycle. *Nature*, *494*(7438), 480–483. https://doi.org/10.1038/nature11897

24. Knoblich, J. A. (2008). Mechanisms of Asymmetric Stem Cell Division. *Cell*, *132*(4), 583–597. https://doi.org/10.1016/j.cell.2008.02.007
25. Lengefeld, J., Cheng, C. W., Maretich, P., Blair, M., Hagen, H., McReynolds, M. R., Sullivan, E., Majors, K., Roberts, C., Kang, J. H., Steiner, J. D., Miettinen, T. P., Manalis, S. R., Antebi, A., Morrison, S. J., Lees, J. A., Boyer, L. A., Yilmaz, Ö. H., & Amon, A. (2021). Cell size is a determinant of stem cell potential during aging. *Science Advances*, *7*(46). https://doi.org/10.1126/sciadv.abk0271
26. Lewis, E. B. (1978). A gene complex controlling segmentation in Drosophila. *Nature*, *276*(5688), 565–570. https://doi.org/10.1038/276565A0
27. Mann, R. S., & Morata, G. (2000). The developmental and molecular biology of genes that subdivide the body of Drosophila. *Annual Review of Cell and Developmental Biology*, *16*, 243–271. https://doi.org/10.1146/ANNUREV.CELLBIO.16.1.243
28. Marianes, A., & Spradling, A. C. (2013). Physiological and stem cell compartmentalization within the Drosophila midgut. *ELife*, *2013*(2). https://doi.org/10.7554/eLife.00886
29. Marin, E. C., Dry, K. E., Alaimo, D. R., Rudd, K. T., Cillo, A. R., Clenshaw, M. E., Negre, N., White, K. P., & Truman, J. W. (2012). Ultrabithorax confers spatial identity in a context-specific manner in the Drosophila postembryonic ventral nervous system. *Neural Development*, *7*(1). https://doi.org/10.1186/1749-8104-7-31
30. Matthews, K. A., Kunte, A. S., Tambe-Ebot, E., & Rawson, R. B. (2009). Alternative Processing of Sterol Regulatory Element Binding Protein During Larval Development in Drosophila melanogaster. *Genetics*, *181*(1), 119. https://doi.org/10.1534/GENETICS.108.093450
31. Micchelli, C. A., & Perrimon, N. (2006). Evidence that stem cells reside in the adult Drosophila midgut epithelium. *Nature*, *439*(7075), 475–479. https://doi.org/10.1038/nature04371
32. Miettinen, T. P., & Björklund, M. (2016). Cellular Allometry of Mitochondrial Functionality Establishes the Optimal Cell Size. *Developmental Cell*, *39*(3), 370–382. https://doi.org/10.1016/j.devcel.2016.09.004
33. Miller, D. F. B., Rogers, B. T., Kalkbrenner, A., Hamilton, B., Holtzman, S. L., & Kaufman, T. (2001). Cross-regulation of Hox genes in the Drosophila melanogaster embryo. *Mechanisms of Development*, *102*(1–2), 3–16. https://doi.org/10.1016/S0925-4773(01)00301-X
34. Ming, G. li, & Song, H. (2011). Adult neurogenesis in the mammalian brain: significant answers and significant questions. *Neuron*, *70*(4), 687–702. https://doi.org/10.1016/J.NEURON.2011.05.001
35. Nagarkar-Jaiswal, S., Lee, P. T., Campbell, M. E., Chen, K., Anguiano-Zarate, S., Gutierrez, M. C., Busby, T., Lin, W. W., He, Y., Schulze, K. L., Booth, B. W., Evans-Holm, M., Venken, K. J. T., Levis, R. W., Spradling, A. C., Hoskins, R. A., & Bellen, H. J. (2015). A library of MiMICs allows tagging of genes and reversible, spatial and temporal knockdown of proteins in Drosophila. *ELife*, *2015*(4). https://doi.org/10.7554/eLife.05338
36. Ohlstein, B., & Spradling, A. (2006). The adult Drosophila posterior midgut is maintained by pluripotent stem cells. *Nature*, *439*(7075). https://doi.org/10.1038/nature04333
37. Ohlstein, B., & Spradling, A. (2007). Multipotent Drosophila intestinal stem cells specify daughter cell fates by differential notch signaling. *Science*, *315*(5814), 988–992. https://doi.org/10.1126/science.1136606
38. Peterson, C., Carney, G. E., Taylor, B. J., & White, K. (2002). reaper is required for neuroblast apoptosis during Drosophila development. *Development*, *129*(6), 1467–1476. https://doi.org/10.1242/dev.129.6.1467
39. Prokop, A., Bray, S., Harrison, E., & Technau, G. M. (1998). Homeotic regulation of segment-specific differences in neuroblast numbers and proliferation in the Drosophila central nervous system. *Mechanisms of Development*, *74*(1–2), 99–110. https://doi.org/10.1016/S0925-4773(98)00068-9
40. Rogulja-Ortmann, A., & Technau, G. M. (2008). Multiple roles for Hox genes in segment-specific shaping of CNS lineages. *Fly*, *2*(6). https://doi.org/10.4161/fly.7464
41. Sánchez-Herrero, E., Vernós, I., Marco, R., & Morata, G. (1985). Genetic organization of Drosophila bithorax complex. *Nature*, *313*(5998), 108–113. https://doi.org/10.1038/313108a0
42. Schmidt, H., Rickert, C., Bossing, T., Vef, O., Urban, J., & Technau, G. M. (1997). The embryonic central nervous system lineages of Drosophila melanogaster: II. Neuroblast lineages derived from the dorsal part of the nueroectoderm. *Developmental Biology*, *189*(2), 186–204. https://doi.org/10.1006/dbio.1997.8660

43. Sen, S. Q., Chanchani, S., Southall, T. D., & Doe, C. Q. (2019). Neuroblast-specific open chromatin allows the temporal transcription factor, hunchback, to bind neuroblast-specific loci. *ELife*, *8*. https://doi.org/10.7554/eLife.44036
44. Siegrist, S. E., Haque, N. S., Chen, C. H., Hay, B. A., & Hariharan, I. K. (2010). Inactivation of both Foxo and reaper promotes long-term adult neurogenesis in Drosophila. *Current Biology : CB*, *20*(7), 643–648. https://doi.org/10.1016/J.CUB.2010.01.060
45. Sood, C., Doyle, S. E., & Siegrist, S. E. (2021). Steroid hormones, dietary nutrients, and temporal progression of neurogenesis. *Current Opinion in Insect Science*, *43*, 70–77. https://doi.org/10.1016/J.COIS.2020.10.008
46. Sousa-Nunes, R., Yee, L. L., & Gould, A. P. (2011). Fat cells reactivate quiescent neuroblasts via TOR and glial insulin relays in Drosophila. *Nature*, *471*(7339), 508–513. https://doi.org/10.1038/NATURE09867
47. Starling Emerald, B., & Roy, J. K. (1997a). Homeotic transformation in Drosophila. *Nature 1997 389:6652*, *389*(6652), 684–684. https://doi.org/10.1038/39500
48. Tan, Y., Yamada-Mabuchi, M., Arya, R., Pierre, S. S., Tang, W., Tosa, M., Brachmannspi-Sup, C., & White, K. (2011). Coordinated expression of cell death genes regulates neuroblast apoptosis. *Development (Cambridge, England)*, *138*(11), 2197–2206. https://doi.org/10.1242/DEV.058826
49. Taylor, B. J., & Truman, J. W. (1992). Commitment of abdominal neuroblasts in Drosophila to a male or female fate is dependent on genes of the sex-determining hierarchy. *Development*, *114*(3), 625–642. https://doi.org/10.1242/dev.114.3.625
50. Truman, J. W., & Bate, M. (1988). Spatial and temporal patterns of neurogenesis in the central nervous system of Drosophila melanogaster. *Developmental Biology*, *125*(1), 145–157. https://doi.org/10.1016/0012-1606(88)90067-X
51. White, K., Grether, M. E., Abrams, J. M., Young, L., Farrell, K., & Steller, H. (1994). Genetic control of programmed cell death in Drosophila. *Science*, *264*(5159), 677–683. https://doi.org/10.1126/science.8171319
52. Yadav, V., Mishra, R., Das, P., & Arya, R. (2024). Cut homeodomain transcription factor is a novel regulator of growth and morphogenesis of cortex glia niche around neural cells. *Genetics*, *226*(1). https://doi.org/10.1093/GENETICS/IYAD173
53. Yu, H. H., Awasaki, T., Schroeder, M. D., Long, F., Yang, J. S., He, Y., Ding, P., Kao, J. C., Wu, G. Y. Y., Peng, H., Myers, G., & Lee, T. (2013). Clonal Development and Organization of the Adult Drosophila Central Brain. *Current Biology*, *23*(8), 633–643. https://doi.org/10.1016/J.CUB.2013.02.057
54. Yuan, X., Sipe, C. W., Suzawa, M., Bland, M. L., & Siegrist, S. E. (2020). Dilp-2-mediated PI3-kinase activation coordinates reactivation of quiescent neuroblasts with growth of their glial stem cell niche. *PLoS Biology*, *18*(5). https://doi.org/10.1371/JOURNAL.PBIO.3000721

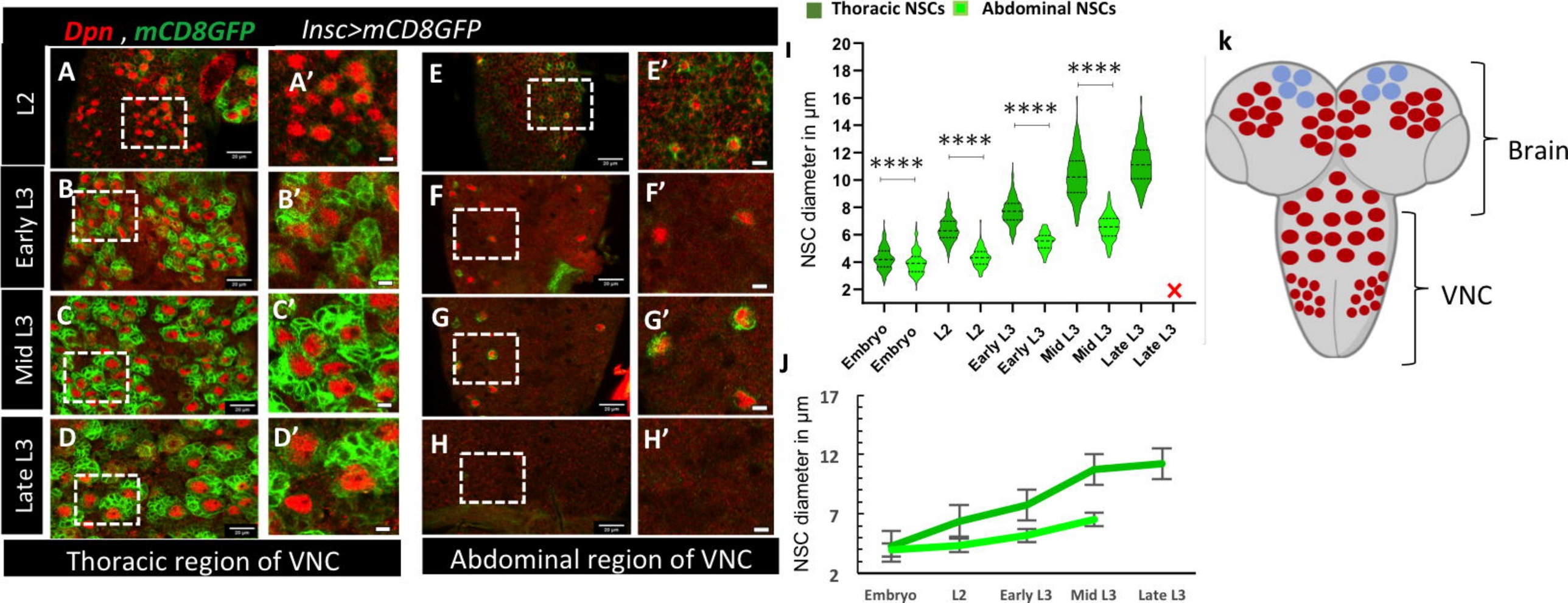
Dpn , mCD8GFP
Insc>mCD8GFP
L2
Early L3
Mid L3
Late L3
A
A'
B
B'
C
C'
D
D'
E
E'
F
F'
G
G'
H
H'
Thoracic region of VNC
Abdominal region of VNC
Thoracic NSCs
Abdominal NSCs
I
NSC diameter in µm
20
18
16
14
12
10
8
6
4
2
****
****
****
****
Embryo
Embryo
L2
L2
Early L3
Early L3
Mid L3
Mid L3
Late L3
Late L3
J
NSC diameter in µm
17
12
7
2
Embryo
L2
Early L3
Mid L3
Late L3
k
Brain
VNC

Insc>mCD8GP

Insc>mCD8GP;abdA RNAi

L2

Early L3

Mid L3

Late L3

A

B

C

D

E

F

G

H

Dpn , mCD8GP

Abdominal VNC region

Control abdominal NSC

abdA RNAi abdominal NSC

I

NSC diameter in µm

20
18
16
14
12
10
8
6
4
2

****
****
****

L2
Early L3
Mid L3
L2
Early L3
Mid L3
Late L3

J

NSC diameter in µm

11
10
9
8
7
6
5
4

L2
Early L3
Mid L3
Late L3

Control thoracic NSCs

Control abdominal NSCs

abdA RNAi thoracic NSCs

abdA RNAi abdominal NSCs

K

control

abdA RNAi

NSC diameter in µm

20
18
16
14
12
10
8
6
4
2

****
****
****
****
****
****

L2 L2 Early L3 Early L3 Mid L3 Mid L3 Late L3 Late L3 L2 L2 Early L3 Early L3 Mid L3 Mid L3 Late L3 Late L3

28-32 hours ALH

42 - 48 hours ALH

68-70 hours ALH

L

L’

M

M’

N

N’

Dpn-GFP , AbdA

o

NSC cell number

200
150
100
50
0

antp
ubx
abdA
abdB

Hox expression at 1hr ALH

P

NSC cell number

150
100
50
0

antp
ubx
abdA
abdB

Hox expression at 24 hrs ALH

Q

NSC cell number

40
30
20
10
0

antp
ubx
abdA
abdB

Hox expression at 48 hrs ALH

A

Cell death pathway in abdominal NSC

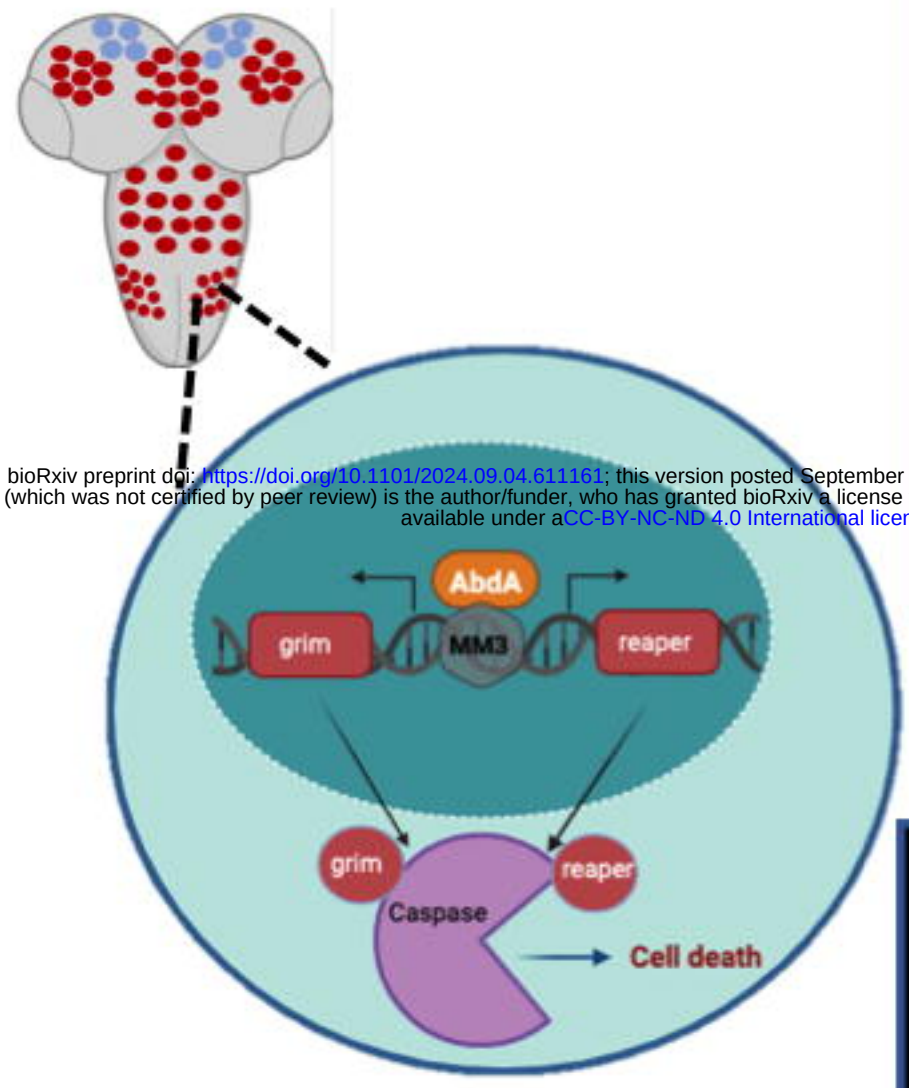

Abdominal region of VNC

Insc>mCD8GFP

Mid L3

B

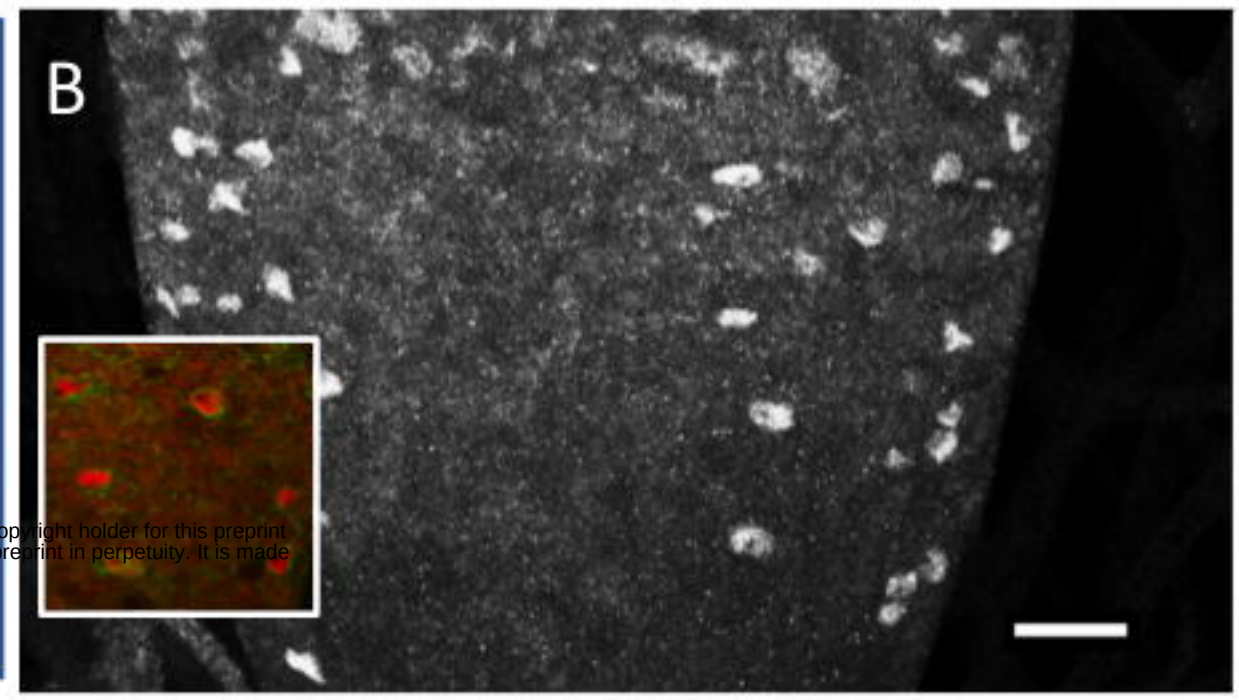

Insc>mCD8GFP,RHGmiRNA

Late L3

C

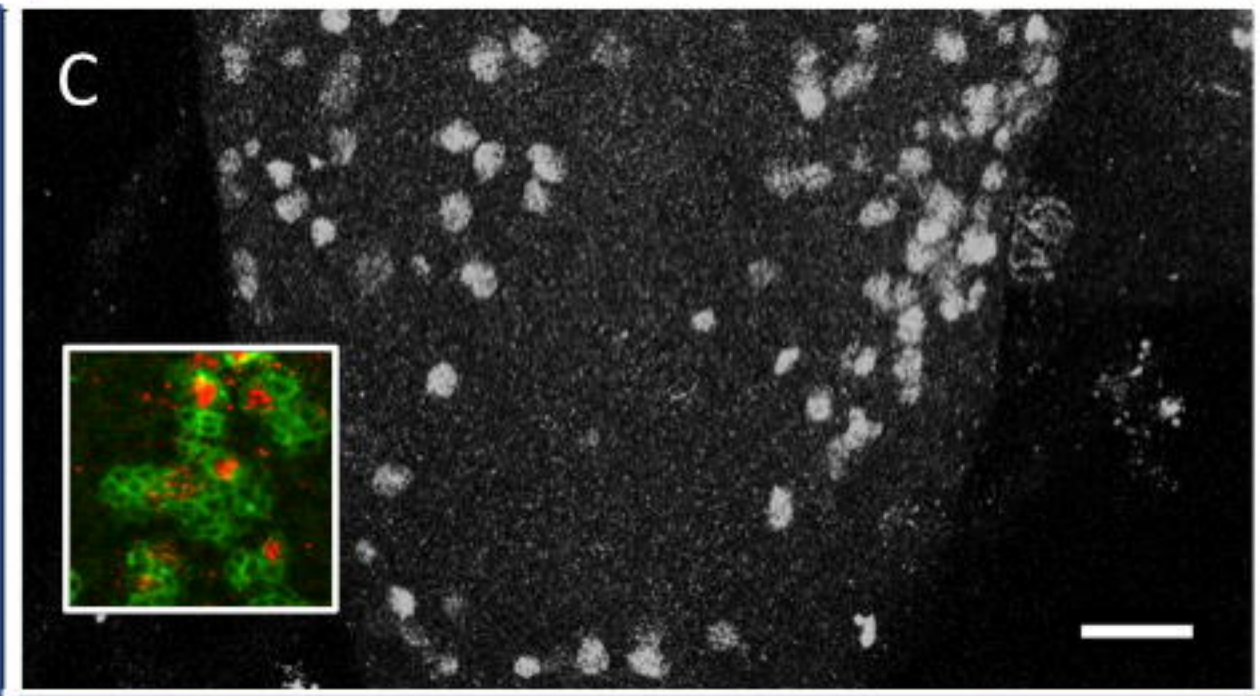

Insc>mCD8GFP;P35

D

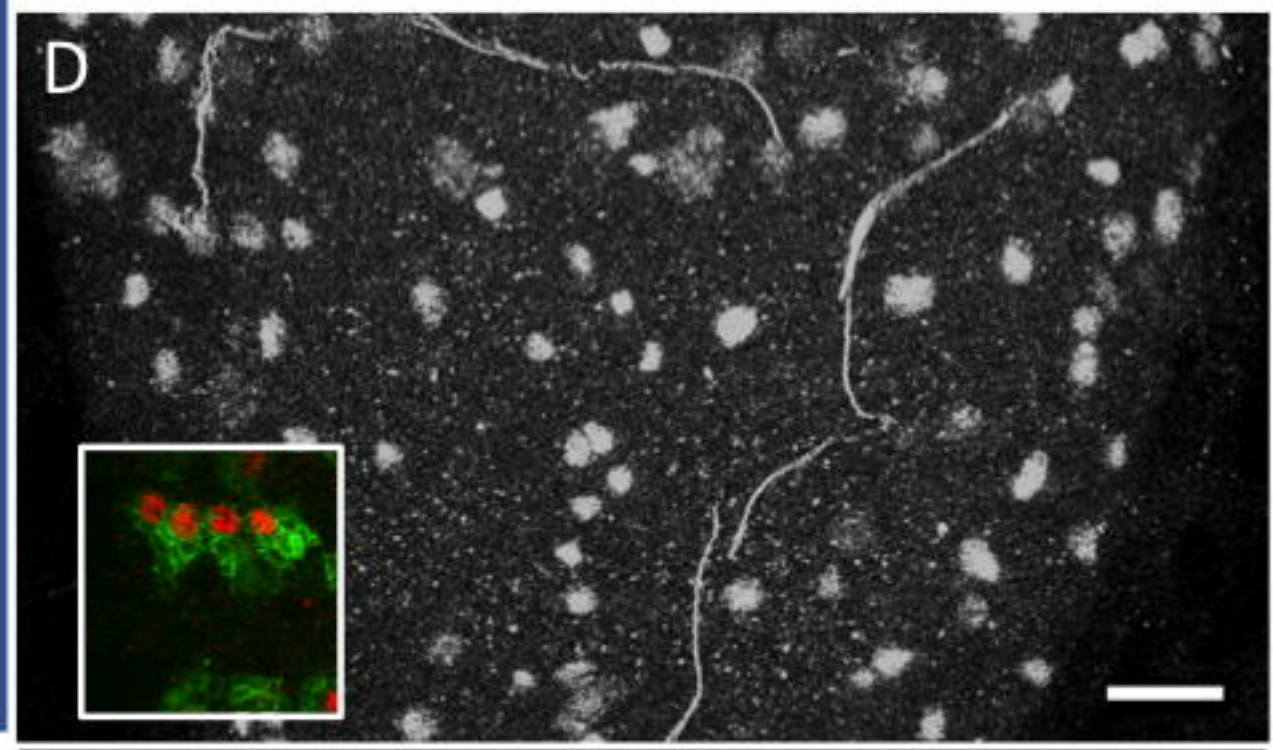

Dpn , Dpn , mCD8GFP

E

Abdominal cells

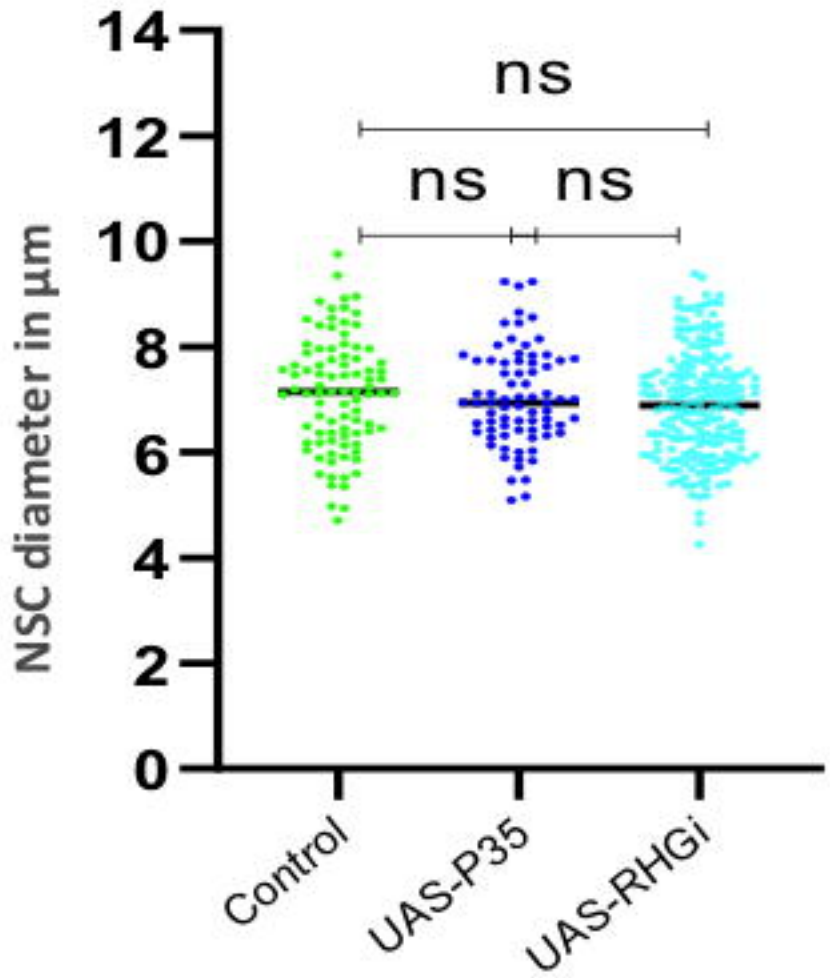

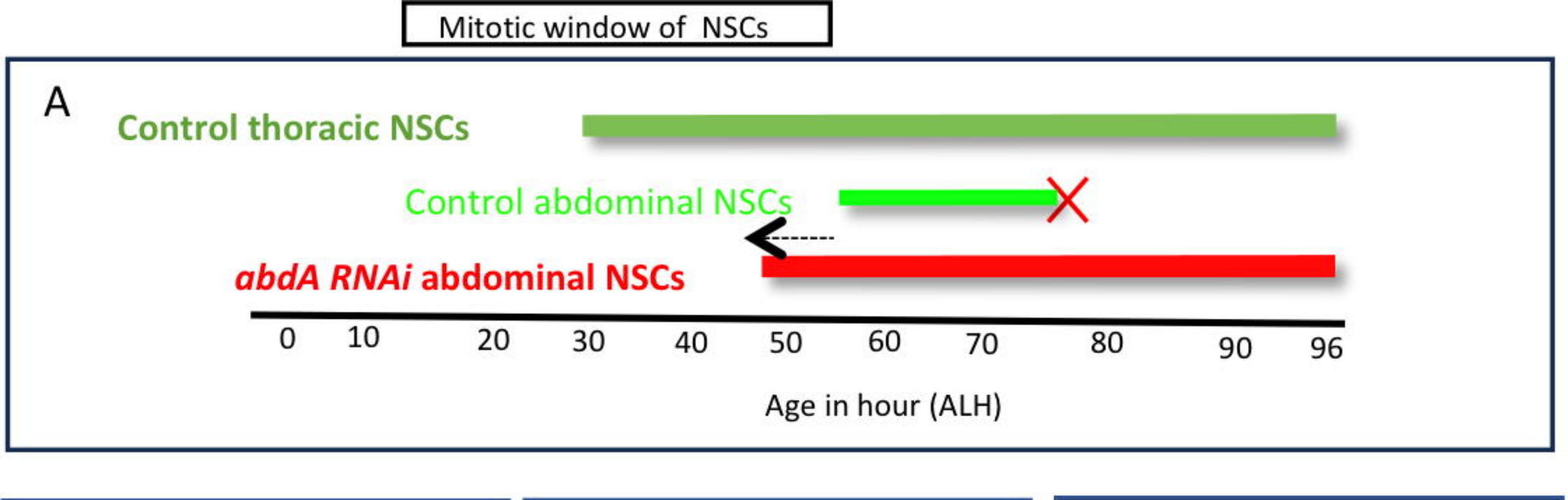

Insc> mCD8GFP | *Insc>mCD8GFP; P35* | *Insc>mCD8GFP;abdA RNAi*

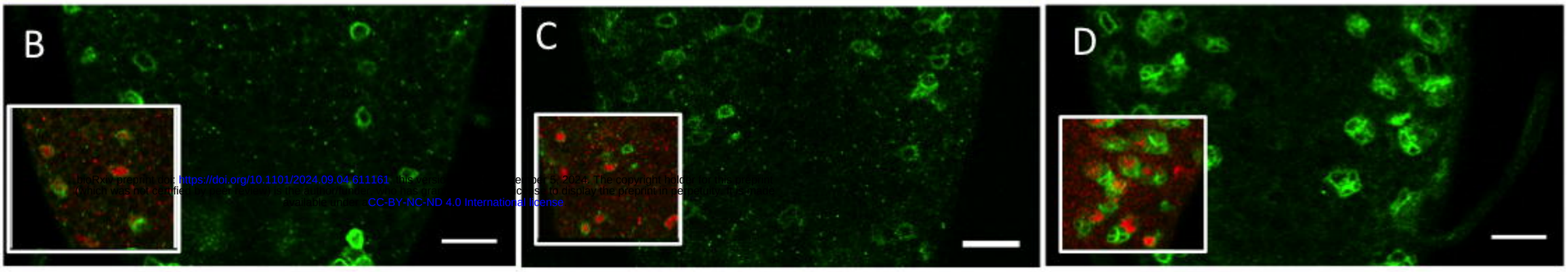

Abdominal region of VNC (48-52 hours ALH)

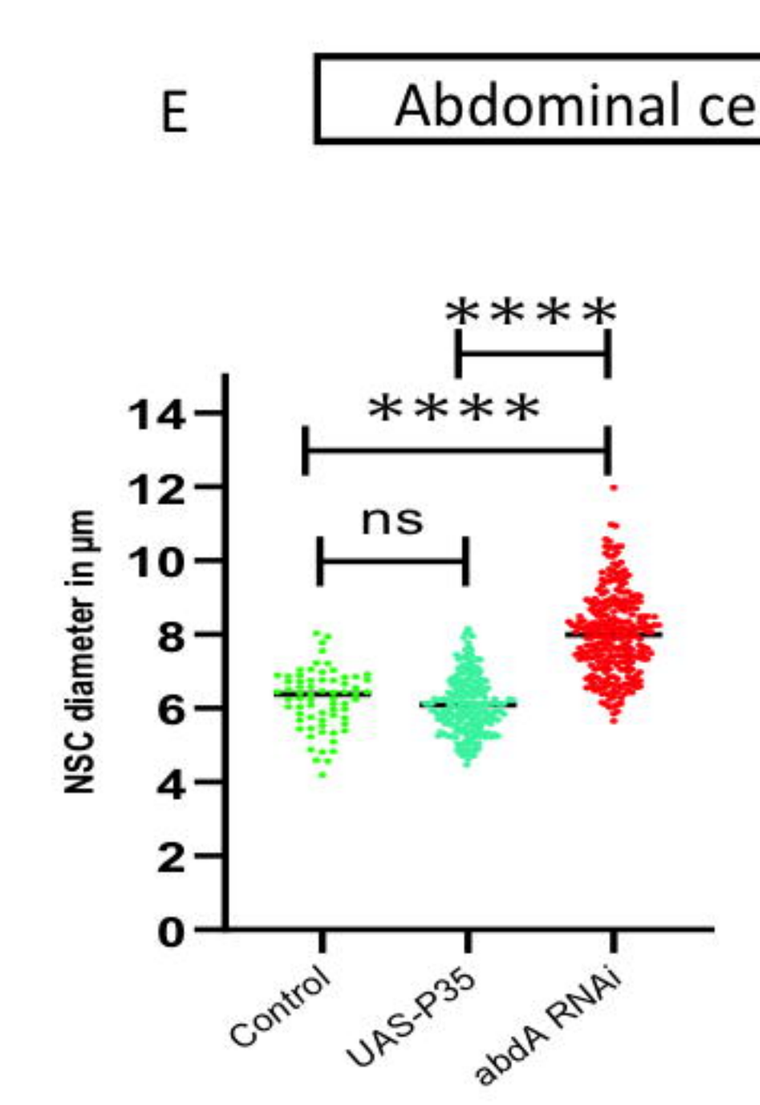

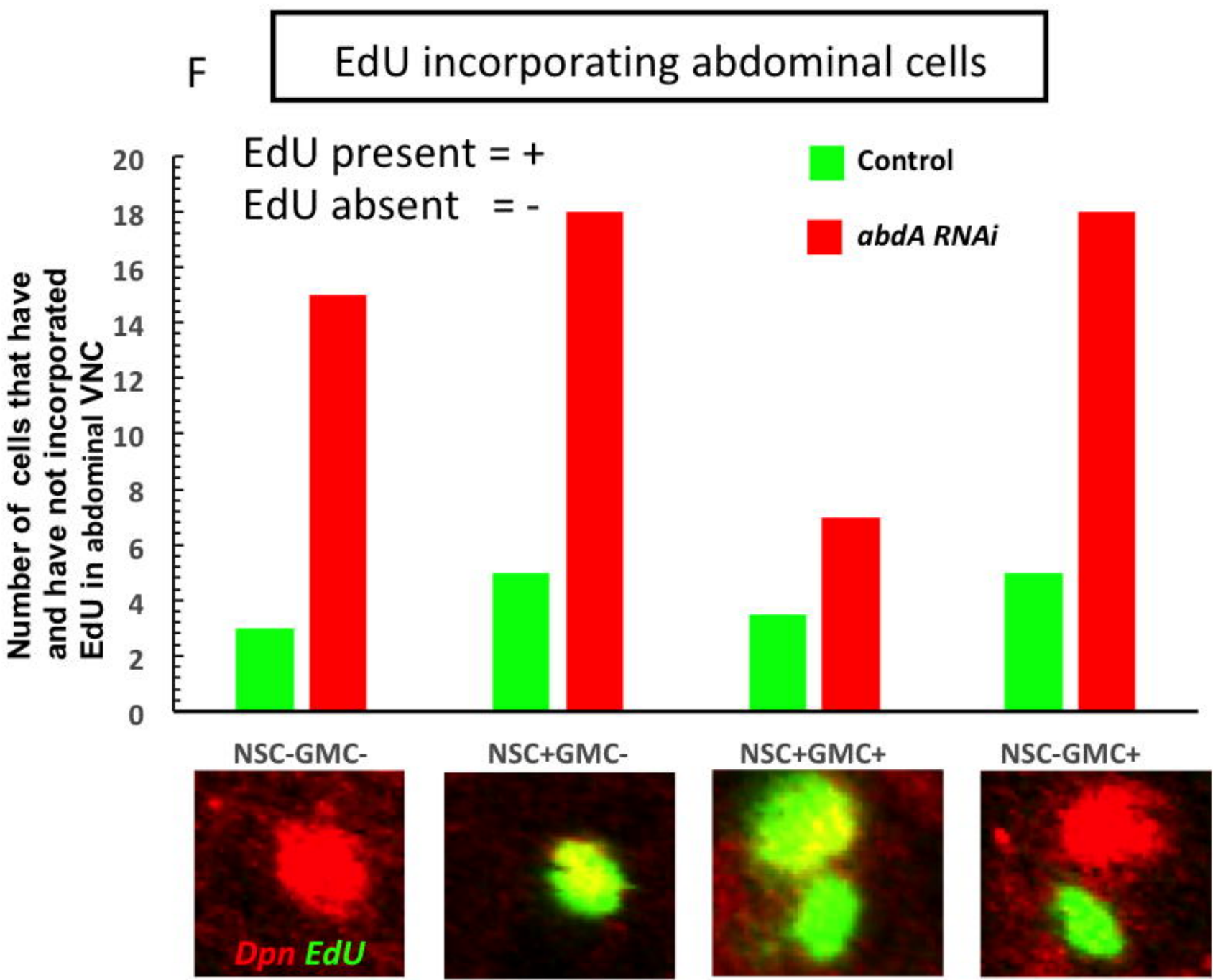

Late L3

insc>mCD8GFP

A

insc>mCD8GFP;P35

B

insc>mCD8GFP,abdA

C

insc>mCD8GFP,abdA;P35

D

30- 35 hours ALH

insc>mCD8GFP

E

insc>mCD8GFP;P35

F

insc>mCD8GFP, abdA

G

insc>mCD8GFP, abdA;P35

H

Thoracic region of VNC

Thoracic NSCs

Late L3

31-35 hr ALH

I

j

K

L

Control thoracic NSCs

UAS-*abdA* thoracic NSCs

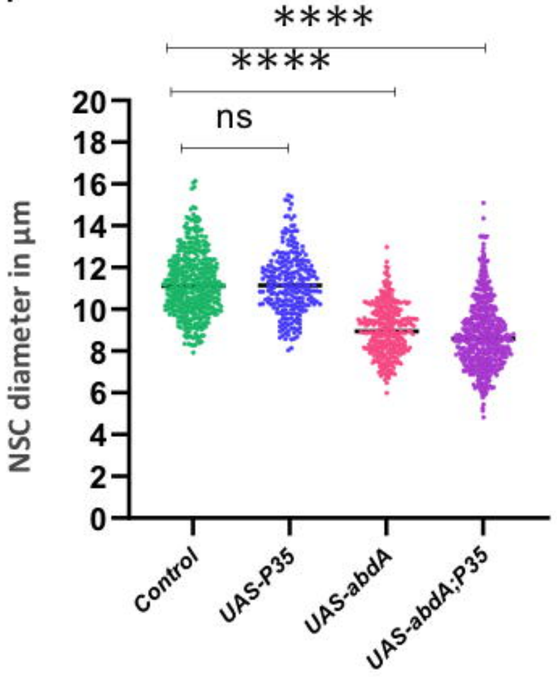

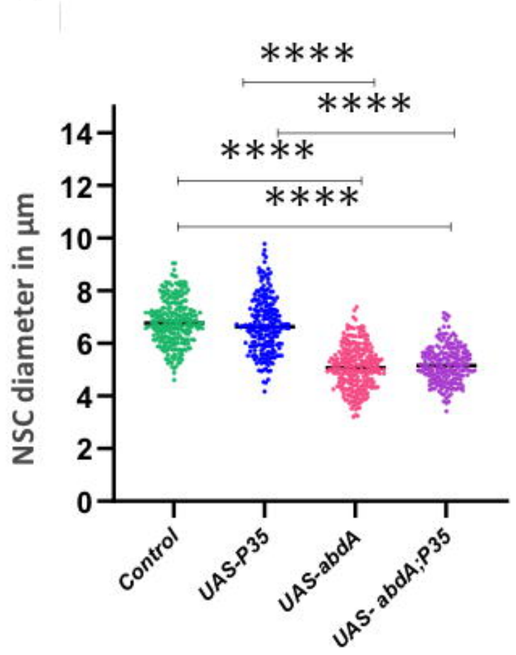

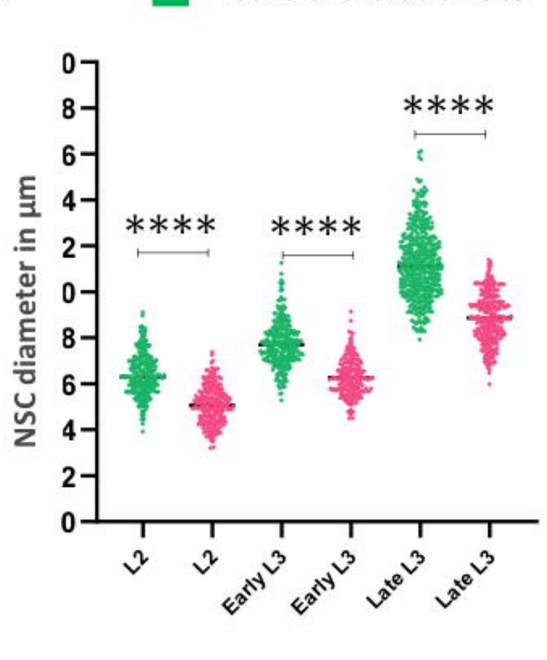

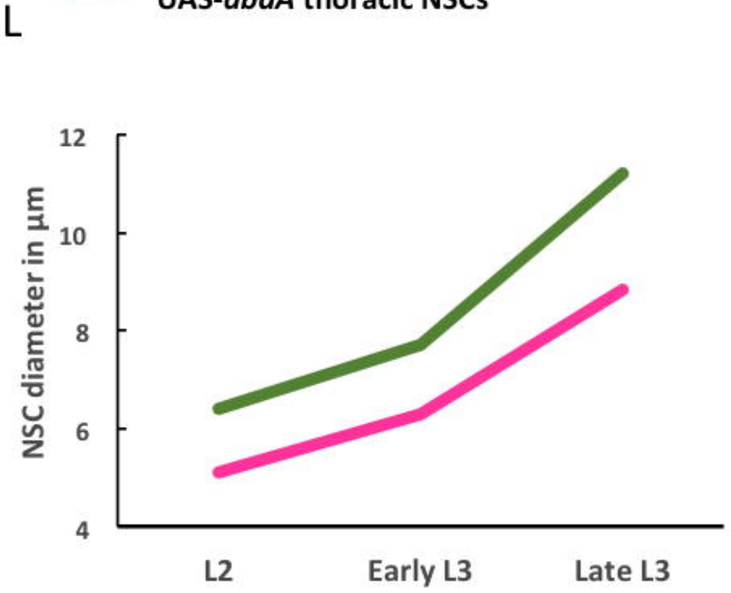

M

Delay in mitotic entry of Thoracic NSCs

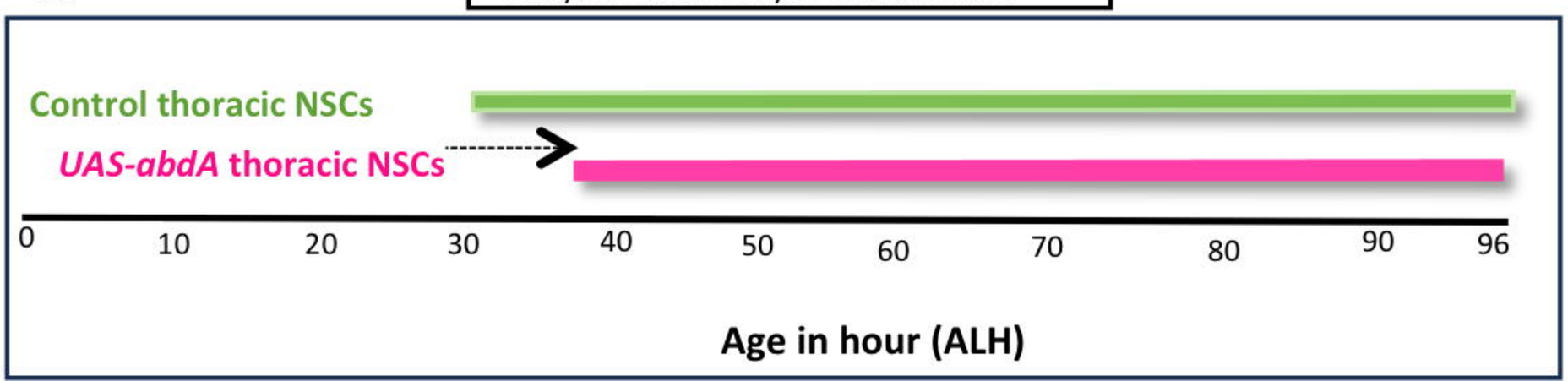

Insc>mCD8GFP

Insc>mCD8GFP;P35

insc>mCD8GFP; abdA RNAi

Standard diet with yeast

20% sucrose without yeast

A

B

C

D

E

F

65 – 68 hours ALH

G

Thoracic NSCs

NSC diameter in µm

20
15
10
5
0

Control *P35* *abdA RNAi* *Control* *P35* **abdA RNAi**

With yeast

Without yeast

H

Abdominal NSCs

NSC diameter in µm

14
12
10
8
6
4
2
0

Control *P35* *abdA RNAi* *Control* *P35* *abdA RNAi*

With yeast

Without yeast

I

Mitotic window of Thoracic NSCs

with yeast diet

without yeast diet

0 10 20 30 40 50 60 70 80 90 96

Age in hour (ALH)

J

Mitotic window Abdominal NSCs

with yeast (control)

with yeast (*abdA RNAi*)

without yeast (control & *abdA RNAi*)

0 10 20 30 40 50 60 70 80 90 96

Age in hour (ALH)

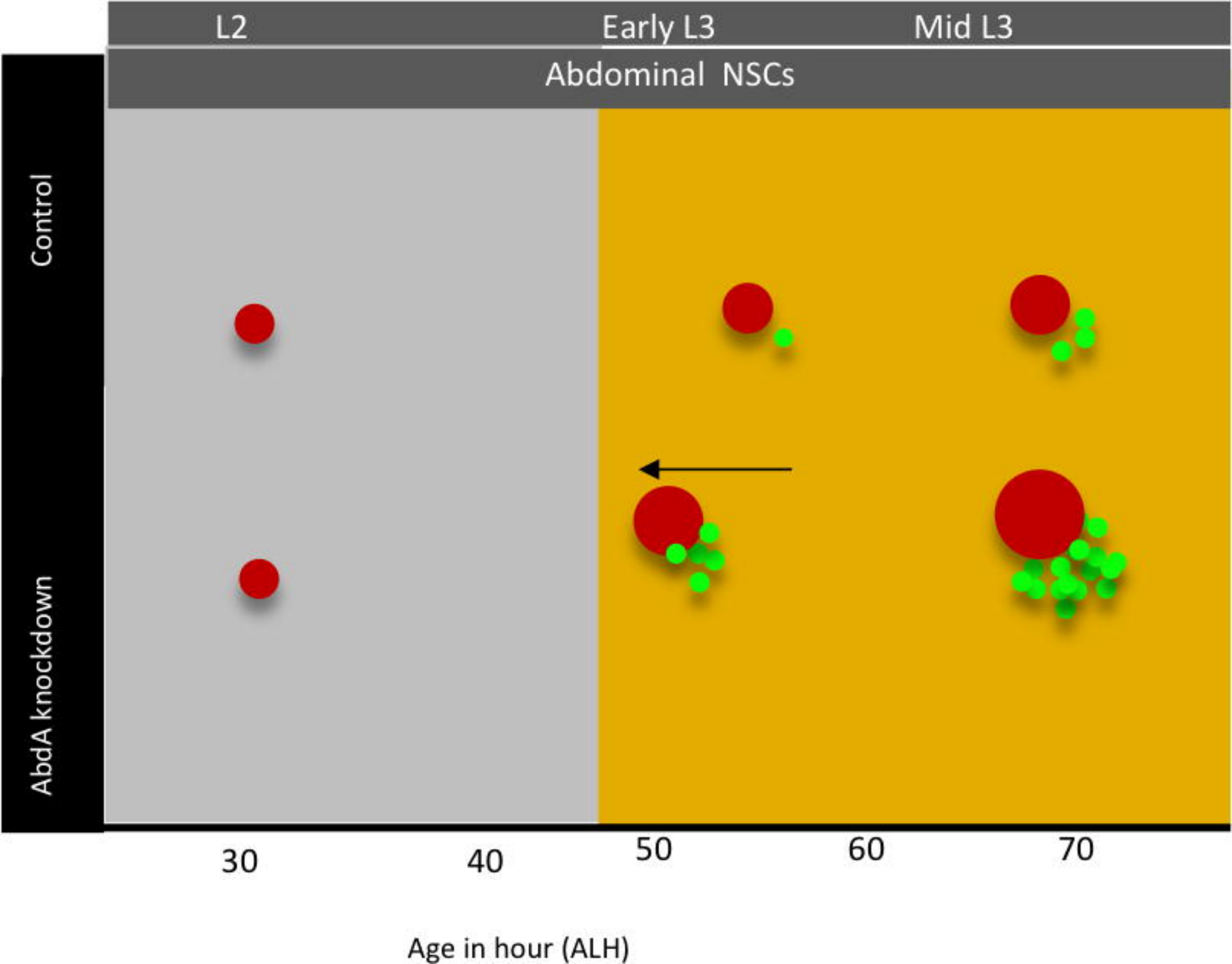
L2
Early L3
Mid L3
Abdominal NSCs
Control
AbdA knockdown
30
40
50
60
70
Age in hour (ALH)